ESD-TR-80-15

12

LEVEL II

Semiannual Technical Summary

Seismic Discrimination

31 March 1980

Prepared for the Defense Advanced Research Projects Agency
under Electronic Systems Division Contract F19628-80-C-0002 by

Lincoln Laboratory

MASSACHUSETTS INSTITUTE OF TECHNOLOGY

LEXINGTON, MASSACHUSETTS

Approved for public release; distribution unlimited.

BLANK PAGES
IN THIS
DOCUMENT
WERE NOT
FILMED

The work reported in this document was performed at Lincoln Laboratory, a center for research operated by Massachusetts Institute of Technology. This research is a part of Project Vela Uniform, which is sponsored by the Defense Advanced Research Projects Agency under Air Force Contract F19628-80-C-0002 (ARPA Order 512).

This technical report has been reviewed and is approved for publication.

FOR THE COMMANDER

Joseph C. Syiek

Joseph C. Syiek
Project Officer
Lincoln Laboratory Project Office

(12)

MASSACHUSETTS INSTITUTE OF TECHNOLOGY

LINCOLN LABORATORY

(6) SEISMIC DISCRIMINATION

(9) SEMIANNUAL TECHNICAL SUMMARY REPORT. 1 Oct 79–31 Mar 80,

TO THE

DEFENSE ADVANCED RESEARCH PROJECTS AGENCY

(10) Michael A. Chinnery

(15) F19628-80-C-0002

(11) 31 Mar 80

(12) 168

1 OCTOBER 1979 – 31 MARCH 1980

ISSUED 6 AUGUST 1980

(18) ESD

(19) TR-80-15

(15) ARPA Order-513

LEXINGTON MASSACHUSETTS

20 16.0 JCB

ABSTRACT

This report describes 19 investigations in the field of seismic discrimination. The contributions are grouped as follows: 6 describe progress in the development of a Seismic Data Center; 3 describe research into seismic algorithms that will be implemented at the Data Center; 7 are concerned with the problem of source characterization using the seismic moment-tensor formulation; and 3 describe recent improvements in our in-house computer systems.

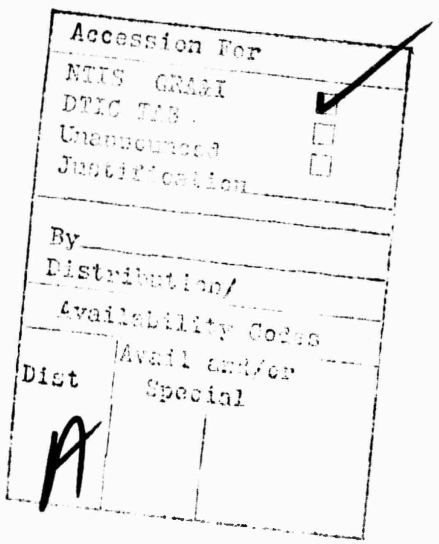

CONTENTS

SUMMARY

This is the thirty-second Semiannual Technical Summary (SATS) report describing the activities of Lincoln Laboratory funded under Project Vela Uniform. This report covers the period 1 October 1979 to 31 March 1980. Project Vela Uniform is a program of research into the discrimination between earthquakes and nuclear explosions by seismic means. An important recent emphasis of the project is in the development of the data-handling and analysis techniques that may be appropriate for the monitoring of a potential Comprehensive Test Ban Treaty, presently under negotiation. During FY 1979, Lincoln Laboratory completed a design for a Seismic Data Center (SDC) that would satisfy this requirement, and the FY 1980 program consists of beginning the actual development of such a data center, and carrying out seismic research with special emphasis on those areas directly related to the operations of the SDC.

The Lincoln Laboratory program is focusing on the development of three subsystems of the SDC – namely the Seismic Analysis Station (SAS), the Local Computer Network, and the Data Base Management System. Initial work has focused heavily on the SAS and, in particular, on a pre-prototype software system referred to as Mod I. This system, running on our in-house PDP-11/45 computer, will allow experimentation and development of new-generation techniques for seismic-data analysis and event bulletin preparation, that will be implemented on the SAS hardware later in the current fiscal year.

The Data Base Management System and the Local Computer Network are in the design and procurement phases. The Data Base Management System design has been refined substantially from that described in the SDC Design report, and now includes a more comprehensive discussion of the indexing of waveform data for rapid retrieval. The Local Computer Network requirements have been formulated in detail, and are presently being procured.

We have begun to examine the seismic algorithms that will be employed in the SDC. Automatic association and location algorithms have been selected for implementation in the Mod I system. As experience in the use of this system grows, we expect to improve or replace these algorithms with better ones. We have continued our interest in detection algorithms, and describe an algorithm that is more sensitive to emergent arrivals. A synthetic program to generate both artificial seismicity and arrivals at a prescribed set of stations is described. This will be used to test and evaluate SDC algorithms.

A major emphasis of the seismic research program has been in the area of source characterization using the moment-tensor formulation. Attempts have been made to understand the generation of anomalous Rayleigh waves by certain explosions at the Eastern Kazakh test site. It is shown that certain components of the moment tensor are very poorly resolved for events with zero depth. Analysis of the anomalous events strongly suggests that they were accompanied by faulting. A new method for the simultaneous inversion of surface-wave data for both moment-tensor and source location is described. This method shows considerable promise for the analysis of special events.

We continue to develop our in-house computer systems. New enhancements to the UNIX operating system, a new graphics package, and the installation of UNIX-compatible Fortran 77 are described.

M.A. Chinnery

SEISMIC DISCRIMINATION

I. SEISMIC DATA CENTER DEVELOPMENT

A. BACKGROUND AND CURRENT STATUS

On 30 September 1979, Lincoln Laboratory completed a Special Internal Report to DARPA/NMRO entitled "Design of a Seismic Data Center." This design study has been reviewed and accepted by DARPA/NMRO as a working basis for the development of a Seismic Data Center (SDC), which will fulfill the following objectives:

(1) Support research and development directed at developing a new generation of seismic-data management and analysis systems.

(2) Develop capability to support current and future data requirements of the DARPA research community.

(3) Provide a test bed for research on more effective seismic analysis methods.

(4) Meet the international and special trilateral data-exchange obligations anticipated under a Comprehensive Test Ban Treaty (currently under negotiation).

(5) Demonstrate new technologies applicable to other seismic missions.

Lincoln Laboratory has been assigned the role of overall technical leadership in the development of this SDC, which will be carried out by Lincoln Laboratory and other DARPA contractors.

The accepted SDC design consists of a set of minicomputers interconnected by a local computer network. For convenience in subsequent discussions, the system can be broken down into seven subsystems (Fig. I-1), namely:

(1) Communications interface and data-logging subsystem, which will carry out all input data reception, reformatting, and logging functions.

(2) Real-time analysis subsystem, which will provide a facility for automatic and interactive analysis of the input data streams in real time, if such a function is required.

(3) Data Base Management Subsystem, which will provide both on- and off-line storage of all raw and processed data within the system, together with appropriate retrieval mechanisms.

(4) Seismic Analysis Station, which will be a single-user interactive waveform and alphanumeric-data-analysis system for both waveform and event processing functions. The final SDC will have several of these stations.

(5) Local Computer Network subsystem, which is a high-data-rate communications network linking all the computers in the system.

(6) General computational support subsystem, which will provide a variety of computational services for software development, certain types of user services, and system monitoring and control.

(7) Research support subsystem, which will carry out all functions related to interactive use of the system (both remote and in-house) by the seismological community.

These subsystems are logical elements, defined in terms of system functions, and should not be regarded as necessarily representing specific hardware components.

Lincoln Laboratory has embarked specifically on the development of the Seismic Analysis Station (SAS), the Local Computer Network, and the Data Base Management Subsystem. Progress in each of these areas is described in the sections that follow.

Hardware for the SAS has been selected and ordered, and delivery is expected within 3 months. In the meantime, we have devoted our main efforts to the development of an interim system that will provide an event-processing capability on alphanumeric arrival data. We refer to this interim system as Mod I in the sections that follow. It is designed, of necessity, to run on our in-house PDP-11/45 computer, and will provide a test bed for the development of data-processing techniques that will be implemented in a more advanced form on the prototype SAS.

The Local Computer Network subsystem has been specified for procurement purposes, and industrial proposals for both hardware and software elements of this subsystem are scheduled to be received in April 1980.

The data management system design has been refined to eliminate some of the duplication of indexing information among the subsystems defined in the special DARPA report. The effect of this design refinement is to simplify the interfaces between the subsystems and to simplify the implementation requirements. Another issue which has been studied in this refinement is efficiency of operation of the waveform data storage. This has led to the modification of the proposed indexing structure of the waveform database. Elements of the parameter database component of this subsystem are being studied during the Mod I development described above. Procurement procedures that may be necessary for this subsystem will be initiated during the remainder of the current fiscal year.

M. A. Chinnery
A. G. Gann

B. THE MOD I INTERIM SYSTEM: OVERVIEW

The purpose of the Mod I system is to provide a test bed for the development of the data structures and data-processing routines that will be implemented on the SAS later in the current fiscal year (upon completion of hardware procurement). Specifically, Mod I consists of a pre-prototype version of the software that will be required for the storage, manipulation, and processing of alphanumeric data. It has been developed on the in-house PDP-11/50 computer at Lincoln Laboratory's Applied Seismology Group.

The basic analyst procedures addressed by the Mod I system are:

(1) Construct an accessible database of seismic arrival parameters,

(2) Subject this database to an automatic association program, to produce a preliminary list of events,

(3) Provide for analyst review and modification of these events, including forming new events from unassociated arrivals, and

(4) Output a completed event bulletin.

As a developmental system, one of the main requirements on the design of Mod I is that it should be easy to add new processing algorithms and procedures. To do this, we have designed a data-access package that allows us to easily change the parameters making up the data files, and we have implemented the various processing steps as separate programs which may be easily modified or replaced. We have made provision for both automatic programs that run unattended on the full database, and for interactive programs that provide the operator with visual feedback after each step. The first version of Mod I is minimal in the functions it provides, but has set the stage for the easy addition of more extensive algorithms and procedures.

The basic elements of the Mod I database are an arrival list, an event list, and an associations list. Each record in the arrival list describes the reception of one phase of a seismic signal at a single station. It contains fields for the station, reported phase, arrival time, amplitude, period, etc. Each record in the event list describes a single event: its latitude, longitude, origin time, depth, error estimates, etc. Each record in the associations list relates one arrival to one event. This includes association-related data such as distance, azimuth, magnitude, and residual. A flag can mark a given association as defining (that is, used in computing the event location) or nondefining. The associations have been placed in a separate list, rather than being incorporated in the arrivals list as is commonly done, to allow the possibility of associating a single arrival with more than one event.

Figure I-2 shows the main software blocks that make up the current Mod I system and how the data flow between them.

Reformat is the program that takes the raw arrival data and transforms them into a Mod I arrival list. The current version of Reformat will handle two types of test data that we have been using to test the Mod I system: data from the International Seismic Month (ISM), and synthetic data produced by a program described in Sec. II-C. After we start receiving ISDE data over the WMO network, Reformat will be expanded to handle that also.

AA is the Automatic Association program. It goes through the full arrival list and attempts to associate arrivals to produce a preliminary event list and associations list. The method used is described in more detail in Sec. II-A.

Select is a program that, given an event number, searches the main database for that event and all arrivals and associations relating to that event. It outputs these as three "per-event" lists that serve as the analyst's working database. All further processing is done on the "per-event" lists until the Accept program is called.

Select has several options. In addition to selecting the arrivals that are currently associated with the requested event, it can also search for and include any unassociated arrivals that have an absolute travel-time residual with respect to the event of less than a specified amount. It can also select only the unassociated arrivals for a particular time period, so that the analyst can then attempt to generate an entirely new event.

Display is a program to display and allow editing of the "per-event" lists. Using Display, the analyst can associate or unassociate any arrival with the event under consideration.

Locate is a program to relocate the event, based on any modifications to the arrivals or associations that might have been made while in the Display program. It has three options for

the initial-event location: it can use the location currently in the database, it can accept a typed-in initial location, or it can use the time and location of the first reported arrival.

Accept is the program which will return the modified "per-event" lists back to the main database.

Par, pev, and px, which are not shown in Fig. 1-2, are programs to print out the arrival, event, and associations lists.

Bulletin, which is also missing from the diagram, is a program to print out the database in standard seismic bulletin format. It lists each event, followed by the arrivals associated with that event.

L. J. Turek

C. THE MOD I DATA-ACCESS PACKAGE

The programs in the Mod I system use a data-access package that has been developed specifically for Mod I. These access subroutines are used to read, write, and search for data stored on disk in a specific list format. Files in this format are called parameter files. In the Mod I context, each of the basic lists – arrival, event, and associations - discussed in the previous section is in the form of such a parameter file.

A feature of the system is that programs which work on a set of parameters will work on any files that contain those parameters, regardless of what other parameters are present. Thus, new parameters can be added to the database without the necessity of recompiling or relinking existing programs. This flexibility can save much effort when a system is in its developmental phase.

When the access subroutine package is used to open a parameter file, it will be given by the user a description of the parameters of interest to the program. It will then set up a mapping from the parameters found in the file to the parameters in a structure provided by the user. Once the mapping is set up, all subsequent reads and writes to the file are accomplished via the user's structure.

A second level of the access subroutine package is the indexing level, which is constructed on top of the basic access level described above. At the indexing level, the user program may choose to build indexes on selected parameters in selected files. Once an index is constructed, it may be used to "look up" the records in the file that contain certain values. Functions provided at this level include:

pirec(EXACT), which searches for a record containing an exact value of the indexed parameter.

pirec(NEAREST), which searches for the record containing the nearest value equal to or greater than the given value of the indexed parameter.

pirecs, which searches for all records containing the exact value of the indexed parameter.

pirange, which searches for all records containing a value of the indexed parameter within the given range.

pistep, which will treat the file as if ordered on the indexed parameter and step forward or backward "n" records.

The design of the indexing level calls for implementing the indexes as B+ trees,* which are ideally suited for both fast searches and the stepping function (which is essential for ordered displays). But in order to begin work on Mod I without waiting for the indexing level to be implemented in its final form, we have provided for an interim version. Currently in use, this interim version has all the functions that will be available in the final version, but has implemented them without indexes, as brute-force searches of the parameter file. When the full implementation is eventually achieved, it can be added to the system with no changes required in the calling programs.

Although these access routines were originally designed for use with Mod I, they are sufficiently general that we expect them to prove themselves useful in several other contexts. For example, the Distributed Sensor Networks project is using them to contain their waveform, spectral, and azimuthal response data output from their signal-processing routines. We also feel that they could form the basis for a general data-handling package similar to the DADS package that was implemented on the PDP-7's.†

L. J. Turek
P. T. Crames

D. LOCAL COMPUTER NETWORK

The previously reported design for the SDC features an architecture utilizing multiple minicomputers interconnected by a local computer network. The local network is needed to provide an effective and efficient means of transmitting data and control information between the various computers which will make up the SDC. This computer network must serve to interconnect the computers very reliably and with a high intercomputer data rate. During this reporting period, a specification for procurement has been drawn up and issued. The proposals of prospective vendors are due in April 1980.

The specific requirements for the multiple-access, broadcast-mode, local-computer-packet network needed for the SDC are:

(1) The network shall provide a signaling speed of 2 Mbps or greater. The design used shall be capable of being extended to 5 Mbps or greater, with no change in host computer software.

(2) The design of the interface shall be modular such that interfacing to a new host requires replacing only the host specific part of the interface.

(3) The initial network shall provide interfaces for the DEC PDP-11 Unibus with DMA transfer of data, in packets with maximum size of not less than 512 bytes, to and from host memory. The initial installation shall provide hardware for 6 host (Unibus) connections.

(4) The network shall be capable of supporting 30 or more hosts. This requires the ability to address at least 30 distinct addresses on the network. This also requires that normal operation be possible with a minimum of 30 hosts physically attached to the communication medium.

---

*D. Comer, "The Ubiquitous B-Tree," ACM Computing Surveys 11, 2 (1979).

†Seismic Discrimination Semiannual Technical Summary, Lincoln Laboratory, M.I.T. (31 December 1972), DDC AD-757560.

(5) The network shall be able to support an "eavesdropping" mode of operation. This means that a host can passively copy a message addressed to a specific address and not perform the acknowledgment protocol. This allows the simultaneous reception of data by multiple hosts, with one host serving as the primary recipient for protocol purposes.

(6) Additionally, the network shall support a broadcast mode where a message is directed to all attached hosts. The broadcast mode does not require positive acknowledgment of each transmission. Normally addressed transmissions shall be positively acknowledged by the addressed host.

(7) The network shall be capable of supporting physical separation between the most distant nodes of at least 1 km. The initial installation will not require separation between the most-distant host to exceed 30 m.

(8) The interfaces shall be fail-safe, i.e., no interface failure can disable more than its attached host.

(9) The interface shall employ traffic sense access to the communications media. That is, the interface shall check for the presence of traffic before initiating any transmission. It should employ collision detection, which is the continued checking for interfering traffic during the period of transmission. If it doesn't use collision detection, it should use a higher signaling speed sufficient to duplicate the performance of the design signaling speed (2 Mbps) using collision detection. If there is any doubt as to the adequacy of the speed of a noncollision detection system, that speed should be supported by analysis using published analytic results comparing carrier sense and collision detection performance in capacity at a fixed expected service delay.

(10) Although it is planned to utilize the network within the confines of a single building, the interface shall employ isolation techniques sufficient to allow attachment of hosts connected to completely separate main power sources, i.e., different utility services – even completely different utility companies.

(11) The physical design shall be such that the host interface can be replaced within 5 min. or switched to a completely separate physical communication medium (previously installed) within 5 min. to service a failure in interface or a communication medium.

(12) The interface shall employ an error detection and control technique at least as good as the CRC technique specified in the International Standards Organization's HDLC (ISO document 3509).

(13) The interface shall have provision for fair access to the local computer net services in the event of extended saturation of load.

(14) The interface should allow the incorporation of a priority scheme to allow favored access to the communication medium by some host in overload conditions.

The preferred design of the local computer network to satisfy these requirements is a set of interfaces to a passive communication medium. Each interface, one for each host computer on the net, would implement the low-level protocols to transfer messages between hosts with a minimum of host processing. The host software would implement higher level protocols to exchange requests and responses between hosts and to transfer logical collections of data between hosts using the lower-level, hardware-implemented protocols.

Unfortunately, there are no commercially available local computer networks that meet the desired characteristics. The procurement currently under way is intended to identify the best compromise of cost and performance, taking into account the required host software as well as the hardware costs, that will satisfy these requirements. As soon as the hardware is chosen, the design of the protocols and the host software to completely realize the needed intercomputer communication capability will be started.

A. G. Gann

E. DESIGN FOR THE INITIAL DATABASE PROTOTYPE

Database design efforts have focused on the initial prototype database implementation. Presented below is an outline of the design and a discussion of the role of this prototype in the overall plan of database development. The initial database module will be implemented as a series of functional units whose interface will allow each individual unit or a selected set of units to be isolated on its own computer. The system will be implemented on a modified UNIX. Initially it will be co-resident with the SAS, but should be capable of being separated therefrom at an early date.

The goals of the initial prototype implementation are to provide a useful, nonredundant implementation for use by other prototype elements of the SDC and to get information which will be useful in building high-performance fully redundant implementations which still provide the same basic functions. In order to fulfill this second goal, the initial implementation will attempt as fine-grained a division into functional units as possible. This will allow freedom in packaging machine functions in later implementations. Isolated functional units will allow multiple active copies of a function to reside in the same host. This will allow numerous experiments to be conducted to determine the suitability of many proposed designs for fully redundant operation, before implementing the final version.

1. Functional Design

Functional units are isolated in such a fashion that they may be placed on separate hosts when connected by a local network. Functional units communicate by means of messages which are passed between units by the kernel, in the same fashion that the local network passes messages between hosts.

Co-residence of multiple functional units on a single host will provide a fruitful environment for testing the system's response to unit or communications failure. Provision of commands to terminate or restart a given unit or disable the communication medium will allow the robustness of the system to be established for large configurations which could not easily be realized if a host were necessary for each functional unit.

Performance predictions can also be supplied by this type of environment by using virtual-time-management techniques similar to those used by the virtual machine emulator.* This will allow determination of performance under a wide range of assumptions.

* M. D. Cannon et al., "A Virtual Machine Emulator for Performance Evaluation," Commun. ACM 23, 71-80 (1980).

2. Waveform Database

The Waveform Database subsystem is one of two sets of intercommunicating functional units, the other being the Parameter Database subsystem. The Waveform Database is responsible for the storage of all waveform data within the system, including reference event data. All users of the Waveform Database will direct their requests to a single point of interface, the index manager. The index manager is responsible for selecting a disk or tape manager which has the data and which will satisfy the request.

3. Index Manager

The index manager maintains an index of all waveform data in the system, whether stored on disk or tape. This allows it to designate the appropriate unit to respond to a waveform read request. The selected unit can then initiate a connection to the requestor and transmit the data independently.

The index manager is also responsible for the allocation of disk space. The index manager's control of disk-space allocation makes it responsible for fielding waveform write requests from the communications interface. Upon receiving a write request, the index manager allocates a disk extent, thereby selecting the disk manager responsible for the spindle on which the extent is to reside. A connection is then set up and data transfer proceeds thereon.

The index manager's control of disk allocation extends to management of the bin tape creation process. Data write requests for each data extent pass through the index manager, and it is therefore in a position to maintain a queue of data to be dumped and to present a manifest containing the location of such data to the tape module so that it may produce a bin tape. Once data have been so dumped, the index manager will keep track of the use of each extent and may thereby deallocate extents on a least recently used (LRU) basis.

4. Disk Manager

The disk manager is responsible for the high-speed transfer of waveforms upon request by the index manager. The disk manager sets up a connection with the original requestor identified by the index manager and then proceeds to transfer the data between the established network connection and the disk. Data transfer proceeds sequentially within a single extent, so no indexing is needed. At the completion of the transfer, the index manager is notified so that further segments may be transferred in a like manner.

5. Tape Manager

The tape manager is responsible for producing and updating bin tapes in response to index manager instructions, and for reading data on bin tapes and reference event tapes back into the system. It is assumed here that other use of tapes will be handled in a logically distinct functional unit. This may be on another machine or possibly as a separate task on the same machine.

6. Parameter Database

The Parameter Database subsystem is responsible for system storage of nonwaveform data. It is layered into two functional units: the file system, which provides a UNIX-type file system as a central storage repository for network users; and the database manager, which uses the underlying file system and provides an object-oriented data-management system.

The file system will be based on the current UNIX kernel file system code. By moving this function into a supervisor address space and making it a server responding to messages from the other units passed to it by the kernel, the basis is laid for a central file repository for the local network. This repository may be used to read or write individual file records or to copy entire files from their canonical version to an SAS or other network user.

The database manager provides an object-oriented data-independent interface, to be used primarily in the handling of event and arrival lists. The searching of the database for objects which have certain characteristics will be performed by the database manager upon command, with the matching objects returned to the caller in a caller-specified format. The precise requirements of the application in this regard have yet to be determined.

D. B. Noveck

F. THE SDC DOCUMENTATION SYSTEM

During the initial design phase of the SDC, it was perceived that an organic procedure was required to assure proper information flow among the designers of the center. This is especially important since some of the designers and implementors of sub-projects are not located at the Applied Seismology Group. Also, a method of exercising a relatively tight overview of the project's progress was desired. An accessible documentation system was seen as an important factor in achieving this objective.

The aim of the documentation system is to have a flexible system which provides a "friendly face" to both the generator and reader of the documents. It should provide the means for easy transfer of information between all personnel in the project throughout the history of the project. We decided to maintain the design, scheduling, progress, and operations documentation on-line, on the Group's general-purpose computers. Nonresident personnel would then be able to access and create documents via the ARPAnet. These computers, of the PDP-11 family, use the UNIX operating system which has been utilized in the past for the implementation of text-handling systems (for example, AT&T has used the system for publication of the Bell System Technical Journal).

The design of the documentation system falls into three main categories:

(1) A storage mechanism for the documents which is organic to the design of the SDC. The UNIX file system was easily tailored to perform this task. A documentation hierarchical file structure was constructed which parallels the overall system design.

(2) A set of commands to easily access and maintain the documentation. A level of protection was required so that documents which numerous people might have to modify would not become cloned, and then modified in parallel; this would result in multiple "up-to-date" versions of the same document.

(3) A method of implementing a set of standards so that the documents of differing authors would have a uniform appearance. It was decided to use the nroff program, a relatively sophisticated text assembly program, to aid in achieving this task.

1. The Hierarchy of the File Structure

The file structure parallels the functional structure of the proposed SDC. The top-level directory is divided into eight sub-directories, six of which are related to the functional separation of the SDC. Each of these contains sub-directories, and not documents. Of the two remaining, one is for documents relating to the SDC, as a whole, and the other is a "catch all" category for random notes which, when generated, didn't seem to fit anywhere. The eight directories are:

oview	executive summary, system status, milestones
comm	communications interface
vsrf	VSC seismic research facility
sas	seismic analysis station
dbs	database system
net	local network
gsc	Lincoln Laboratory seismic research facility
notes	system-wide information not in any other category

Within each of the six functional task directories, there are five sub-directories:

oview
if
fcn
dgn
notes

For each task, files in the "oview" directory store the current status and milestone schedule for that task as well as a brief summary of the purpose and design.

The "if" directory contains one or more documents which (together) constitute the interface specifications for the interfaces to other elements in the system. The "fcn" directory contains files which constitute the functional specification of the overall subsystem and each separately identified subdivision of the subsystem.

The "dgn" directory contains files documenting the design of each part of the subsystem. These documents give the higher level design considerations for the programs. The "notes" directory is used (at all levels) to catch thoughts and ideas which are not readily categorized into the above categories. Some of these may be moved later into the regular categories, others may cause new categories to be added, and others may be dropped after discussion and further thought. The purpose of this "catch-all" category is to ensure that no idea is lost for lack of a category.

It is anticipated that each directory will have a person who is responsible for maintaining the integrity of the directory. This is primarily ensuring that all files in the directory are consistent and properly maintained.

2. Documentation Maintenance Commands

The following is a quick overview of the commands used to access and maintain the documentation in this system. The commands are reserve, distribute, runoff and look, and since.

Reserve	Makes a copy of the named file available for exclusive access by a user. The previous version of the file (if any) remains accessible by all users for viewing only.
Distribute	Installs the new version of a file for access by all users. The previous version is archived in a special directory for later copy to magnetic tape. Thus, a complete audit trail of versions of a file is available.
Runoff	Reformats a file from the internal format to the display format. The output is via the UNIX Standard Output, hence is available for processing by filters or filing via shell options. A special variant of runoff, called look, is used if and only if the file is currently reserved to the user, while runoff will give the publicly accessible version at all times.
Since	Gives a list of all files changed in the specified number of days. A specified directory or the current directory and all subsidiary directories are scanned to determine all files which have been changed (or created) within the past specified number of days.

3. Document Production

In order to have a uniform appearance for the SDC documentation, we will use a standard documentation method. This will enable us to distribute up-to-date versions which, if we maintain the documentation database, will accurately and clearly reflect the current status and future of the SDC. In addition, it will enable us, by simply joining relevant sections, to produce whatever reports are required.

An expository flexible format is required for transmitting conceptual information. The author's mind view of the concept has much to do with the way in which it should be presented. Minimizing the transformation from the creator's mind to the page will tend to ease the documentation process for the author, and allow the concepts to be more readily grasped. Using a common documentation package, which gives us the flexibility required, will both ease the transition from mind to media and provide a uniform appearance to the documentation.

We will use the nroff program which is controlled, from within the text stream, by a detailed group of commands. These commands provide the means of formatting the document to be displayed. The commands can be grouped together into interactive packages called macros.

We use a subset of the standard -ms macro package, to which additions have been made to fit our needs. Using a common documentation package, and a few guidelines, gives the documentation a standard appearance without being a burden on the authors, and gives the flexibility required.

4. Initial Results

The initial use of the documentation system has been very favorable. It was first used to document the documentation system. This "shakedown" process resulted in modifications to

components of the system and, hence, to concomitant revision of the documentation system's documentation. The system is now stable. Existing SDC documentation, which was developed outside the documentation system, is now being moved onto the system.

R. S. Blumberg
A. G. Gann

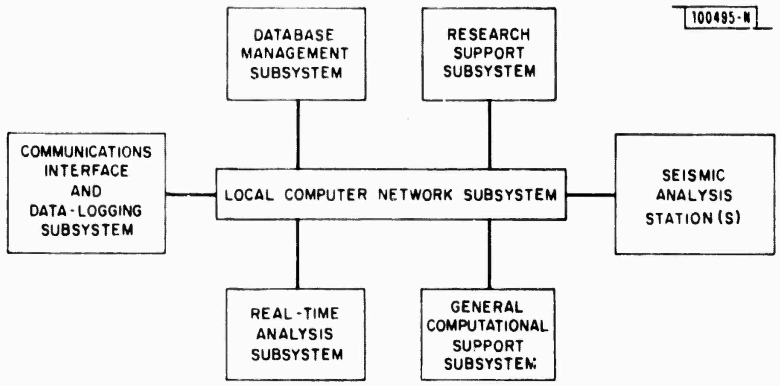

Fig. I-1. Functional subsystems of SDC. These may not correspond to hardware components, since in some possible configurations several functions may be carried out on same computer.

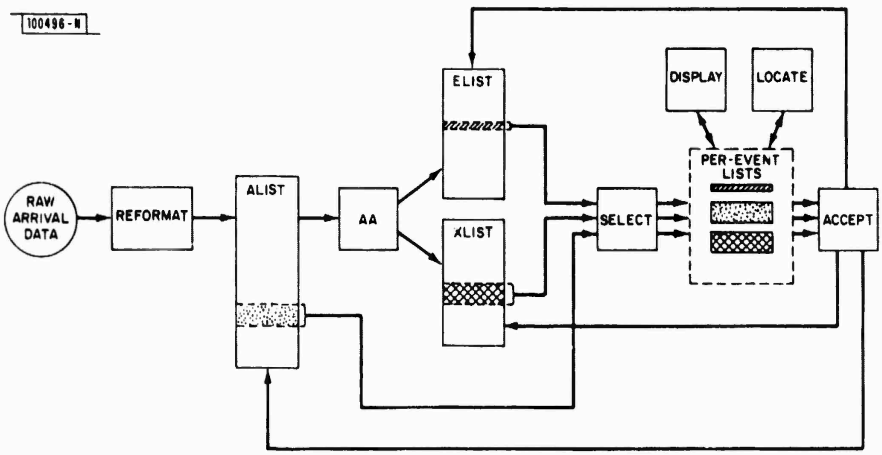

Fig. I-2. Software elements of Mod I interim system.

II. SEISMIC ALGORITHMS

A. AUTOMATIC ASSOCIATION

One of the main goals of the SDC is to produce a list of earthquake locations from a list of seismic-wave arrival times. This process is known as "association," since sets of incoming arrivals must be associated with particular epicenters. About five different automatic-association methods have been developed by various seismic institutions. Unfortunately, none of the methods has established their superiority over the others, and automatic association is thus an area of active research. The following is a progress report on the automatic-association method currently being investigated by the Applied Seismology Group at Lincoln Laboratory.

One of the major problems in automatic association is due to the fact that earthquakes may occur at nearly the same time anywhere in the world. For example, for the International Seismological Month (ISM) about 30 percent of the events overlap in time. Thus besides locating the earthquakes from the arrival times, which by itself is not a simple task,[1] one must decide which set of arrivals should be assigned to which earthquakes.

The association problem can be represented as the following combinatorial optimization problem: Find X, the set of earthquake locations, which minimizes

$$\sum_{x_j \epsilon X} P(x_j, A_j) + \alpha |X| + \beta |U|$$

where A_j is the set of arrivals associated with location x_j, $P(x_j, A_j)$ is the cost of associating location x_j with the set of arrivals A_j, α and β are appropriate constants, and U is the set of unassociated arrivals. The second and third terms essentially apply Occam's razor by trying to associate as many arrivals as possible, and at the same time keeping the number of events as small as possible. In words, this equation says we want to find the smallest number of earthquakes which best explains as many arrivals as possible.

Combinatorial optimization problems are usually quite difficult to solve, and this one has the additional complication of errorful data. Normally, suboptimal heuristic solutions are found using a form of the hypothesize-and-test paradigm. A small subset of arrivals (3 to 5) or one or more array measurements is used to determine a hypothetical epicenter. If enough other arrivals agree with this epicenter, it is declared an event and the arrivals are associated with it. This process is then repeated for any remaining unassociated arrivals. Although this procedure is suboptimal, it appears to produce about 80 percent of the events that an analyst would produce with an acceptable false-event rate (G. Dumphy of USGS, personal communication).

1. The Method

The initial version of the automatic-association program (AA) was designed to utilize only P and PKP arrival times. This simplifies the design somewhat, but still provides a useful program (90 percent of the ISM arrivals are P or PKP arrivals). Additional information such as amplitude, later phases, and array measurements can be incorporated into the algorithm later on without much difficulty.

The AA takes two lists as input – a list of arrivals and, optionally, a preliminary list of events. The output of AA is a list of events and their associated arrivals.

If a preliminary event list is available, arrivals are matched to events in the list before new events are searched for. In this way, any external event information can be used, or any arrivals missed during a previous AA run can be assigned to the appropriate event during a later AA run.

When searching for an event, the AA inspects each unassociated arrival in turn. If this arrival (called the key arrival) is consistent with enough other arrivals, it is used to guide a search for an event (see below). Arrivals are temporarily allowed to be associated with any number of events. Later on, an "event critic" stage is used to remove multiple associations and redundant events.

The event critic inspects each arrival and assigns it only to the largest event with which it associates. Any events which no longer have enough associated arrivals are discarded. Thus, the critic acts as a form of Occam's razor. Typically, a discarded event is caused by a false alarm which fortuitously combines with several real arrivals to produce a bogus event. This critic step is vital because it provides AA with a more "global" viewpoint than it would get from a simple left-to-right pass over the arrival list. Without it, many false events can be produced and true events missed.

To search for an event, a circular grid pattern of epicenters is placed around the location of the station corresponding to the key arrival as shown in Fig. II-1. The origin time at each epicenter is chosen as if the key arrival had originated from that spot. The arrivals are then matched against each hypothetical epicenter. An arrival is associated with an epicenter if it matches it within a specified tolerance which depends on the grid spacing. The epicenter which agrees with the most arrivals (or has the lowest cost in case of a tie) is used as the center of further circular search with a reduced grid spacing. The process is repeated until either too few arrivals remain associated or a sufficiently accurate epicenter is obtained. This technique is similar to one used by Snell.[2]

One advantage of this technique is that it simultaneously associates arrivals to an event and produces a location for the event. Also, it avoids some of the problems found by traditional location methods when using errorful arrival data.[1]

2. Results

The testing of association algorithms must be done with care since the test data can exert a strong and unnoticed influence on the development of the algorithm. The AA will be tested on both actual seismic data from the ISM and synthetic seismic data. The ISM data set is particularly valuable because it has been carefully associated by seismic analysts and contains over 40,000 arrivals from nearly 1,000 events.

The preliminary results on a little over 800 ISM arrivals is quite encouraging. Table II-1 compares how arrivals are interpreted by the ISM analysts and by AA. For example, the table

TABLE II-1

APPLICATION TO ISM ARRIVAL DATA. COMPARISON OF AUTOMATIC AND MANUAL ARRIVAL ASSOCIATIONS (PERCENT)

		AA	
		Unassociated	Associated
ISM	Unassociated	30.1	9.7
	Associated	5.1	55.2

TABLE II-2

COMPARISON OF EVENTS FOUND BY AA WITH THOSE FOUND BY THE ISM ANALYSTS

	Number	Percent
MATCH	20	62.5
NEW	5	15.6
SPLIT	7	21.9
MERGE	4	12.5
MISS	1	3.1

shows that 5.1 percent of the arrivals associated with events by ISM analysts remained unassociated after processing by AA.

Table II-2 compares the events found by ISM analysts and by AA. The terms in the left-hand column have the following interpretation:

MATCH — The set of associated arrivals were either unassociated by ISM analysts or were associated to the same event by ISM analysts.

NEW — The associated arrivals were mostly unassociated by ISM analysts.

SPLIT — Arrivals from one ISM event were split into multiple events by AA.

MERGE — The set of associated arrivals came from more than one ISM event.

MISS — The ISM event was completely missed by AA.

These preliminary results are encouraging; only one small event (six arrivals) was missed by AA and over five additional events were found. Three of these events had eight or more associated arrivals.

K. R. Anderson
N. S. Snell

B. AN IMPROVED DETECTOR FOR EMERGENT ARRIVALS

Most proposed detectors employ the Z statistic to compare the average power over a short window (~1.5 sec) against a threshold. To make selection of this threshold easier, the short-term average power (STAP) is normalized to Z using Eq. (II-1):[3]

$$Z = (STAP - MUstap)/SIGMAstap \quad . \tag{II-1}$$

Therefore, Z has a mean of zero and a standard deviation of one. MU and SIGMA are the long-term properties of the STAP and are given initial value during detector startup. They are updated using Eqs. (II-2) and (II-3):[3]

$$MUn+1 = (1 - E) * MUn + E * STAPn \tag{II-2}$$

$$SIGMAn+1 = (1 - E) * SIGMAn + E * (STAPn - MUn) ** 2 \quad . \tag{II-3}$$

For a given startup population N, E = 1/N.

Our detector, as well as the SRO detector, is a Z statistic detector. In order to accurately test the performance of our detector we acquired 6 h of continuous broadband data from the Albuquerque, New Mexico SRO (ANMO). These data were filtered to exactly simulate a short-period (SP) record. The continuous SP record was then 3-pole Butterworth bandpass filtered from 0.5 to 2.0 Hz, the same band used by the SRO detector.

We now had a way to directly compare the SRO detector with other detectors (human or machine). Human analysis of the 6-h record showed that the SRO detector was unable to pick up all emergent signals. These emergent signals are not small. The problem is that slowly emergent signals appear to the detector as would a slow increase in noise. With each slightly higher value for the STAP, the values of MU and SIGMA are pulled up. Eventually the whole signal is passed over, MU and SIGMA are now contaminated with signal, and the detector is less sensitive for a while. To trap these emergent signals, we introduced a time lag between the STAP being tested and the STAP used to update MU and SIGMA.

Figure II-2 shows that, with the SRO detector at point B, MU and SIGMA are already contaminated with signal. This being the case, there is little chance of a detection by point C. With the lag introduced, when the detector is at point C the values of MU and SIGMA have only been updated to point A. This allows detection of emergent signals as small as the smallest impulsive signals detected. The time lag used should not be too long since noise levels can rapidly increase over a short period of time, as with the passage of atmospheric fronts. By trial and error, we found the optimum value of the lag to be 13 sec.

An example of an emergent signal that the SRO detector missed, which was picked up by our detector, is given in Fig. II-3.

It is worth noting that this increased sensitivity to emergent signals was not accompanied by an increase in false alarms.

M. A. Tiberio
R. G. North

C. GENERATION OF A SYNTHETIC ARRIVALS LIST

Two programs have been written – the first of which generates a synthetic list of events, and the second of which computes the arrivals from these events seen at a prescribed network of stations. The purpose of these programs is to provide a systematic method for the evaluation of association and location algorithms. Programs such as this have been written before, but are described here since the choice of parameters used is rather subjective.

The synthetic events list produces a set of events with approximately correct geographical distribution, depth distribution, and frequency-magnitude characteristics. The latter are computed using the frequency-moment relation proposed by Chinnery and North,[4] and the moment-magnitude relations of Chinnery.[5] M_s and m_b are computed from the moment value stochastically, to allow for a range of possible source mechanisms. The number of events listed during a given time period (say, 1 day) is controlled by a threshold moment value. Random numbers are used extensively, so that each run of the program generates a different event list.

One such event list for a single day is illustrated in Figs. II-4 and II-5. Figure II-4 shows the geographical distribution of the 226 events on this list. The moment threshold chosen was 20.0 dyn-cm, which corresponds roughly to $m_b = 3.3$. The frequency-m_b plot for these events is shown in Fig. II-5. The "b-value" of 0.95 is very typical for real events. In this list, there were 3 events with $m_b \geq 5$, and 36 events with $m_b \geq 4$. This corresponds to about 13,000 events per year with $m_b \geq 4$, which is probably a reasonable estimate.[6]

The arrivals program computes P-wave arrivals, and some later phases, at a network of stations. For simulation purposes, the network used for testing consists of 50 globally distributed real stations. Station amplitude biases (North[7]) and travel-time anomalies (Dziewonski[8]) are included. Each station is assigned an average noise level, and (in the present version of the program) is assumed to have an infinite dynamic range. The amplitude of each event at each station is computed, including a Gaussian component to simulate scattering, and an arrival is declared when the signal amplitude is substantially above the noise level. Travel times are computed from standard tables, with a Gaussian random component added to simulate regional variations. A variety of additional complications include removing each station from service for 1 h per day, and occasional operator errors in both depth phase identification and timing. Because of the random quantities, each arrivals list from a given events list is different.

A typical arrivals list produced from the 226 event list mentioned above contained 454 P arrivals and 69 later phases. Seventeen events had at least 5 arrivals, and could therefore (in principle) be associated into events. Approximately 25 percent of the arrivals were from events with less than 5 arrivals and, in practice, would presumably be unassociated. Smaller local events, not included in the event list, would presumably increase this to about 50-percent unassociated arrivals, which is commonly observed. One immediate conclusion is that identification and removal of small local events should, if possible, be carried out before the process of event association.

Efforts to make the final arrivals list more realistic are continuing. Swarms and aftershock sequences will be added, and station noise levels and dynamic ranges refined. The programs will be used to test automatic-association algorithms, and to assess the error bounds generated by location programs. They will also be used to examine the characteristics of existing catalogs such as that issued by the International Seismological Center.[5]

M. A. Chinnery

REFERENCES

1. K. R. Anderson, "Automatic Processing of Local Earthquake Data," Ph. D. Thesis, Department of Earth and Planetary Sciences, M.I.T. (1978).
2. N. S. Snell, "The Detection Association Processor," Texas Instruments Report ALEX(01)-TR-77-06 (1977).
3. M. J. Shensa, "The Defection Detector – Its Theory and Evaluation on Short Period Seismic Data," Texas Instruments Technical Report ALEX(01)-TR-77-03, Section II, 1 (November 1977).
4. M. A. Chinnery and R. G. North, "The Frequency of Very Large Earthquakes," Science 190, 1197-1198 (1975), DDC AD-A024236/2.
5. M. A. Chinnery, "Measurement of m_b With a Global Network," Tectonophysics 49, 139-144 (1978), DDC AD-A065031/7.
6. J. F. Evernden, "Study of Regional Seismicity and Associated Problems," Bull. Seismol. Soc. Am. 60, 393-446 (1970).
7. R. G. North, "Station Magnitude Bias – Its Determination, Causes, and Effects," Technical Note 1977-24, Lincoln Laboratory, M.I.T. (29 April 1977), DDC AD-A041643/8.
8. Seismic Discrimination Semiannual Technical Summary, Lincoln Laboratory, M.I.T. (31 March 1979), DDC AD-A073772/6.

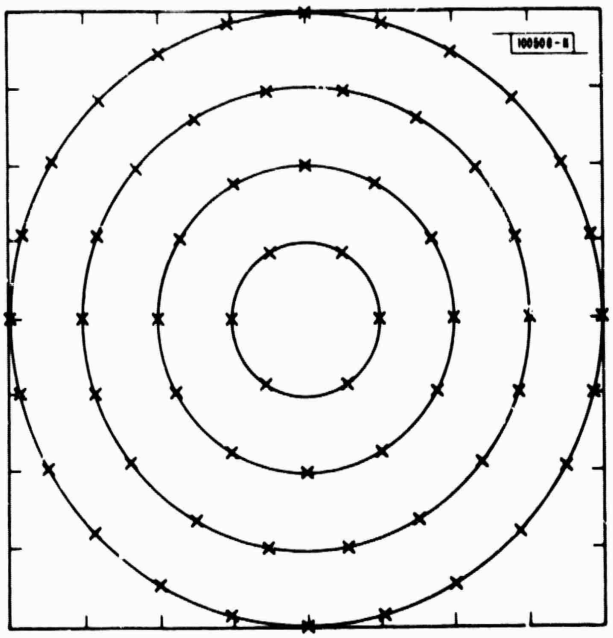

Fig. II-1. In the association algorithm discussed in text, after a key arrival is identified at a particular station, a grid of trial epicenters around that station is used to search for a best event solution. Trial epicenters are arranged in a circular pattern as shown here. Typical circle spacings are 5° to 10°.

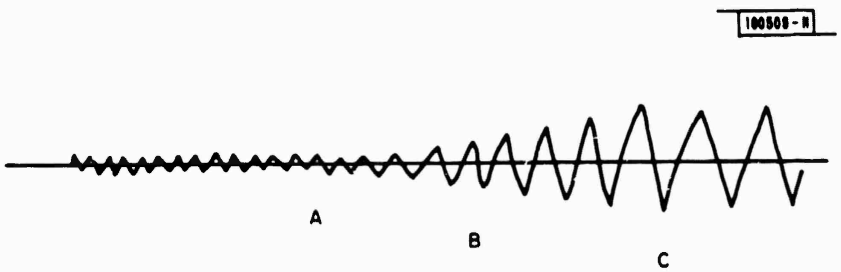

Fig. II-2. Schematic of emergent arrival.

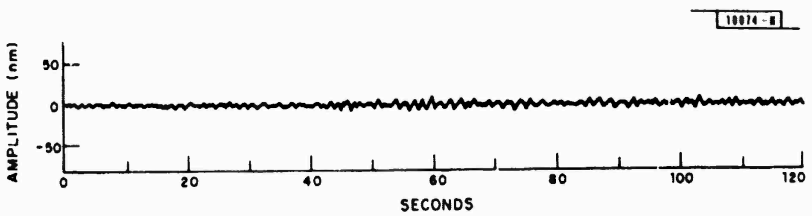

Fig. II-3. Example of emergent arrival at ANMO which was detected only after introduction of lag in determination of MUstap, SIGMAstap.

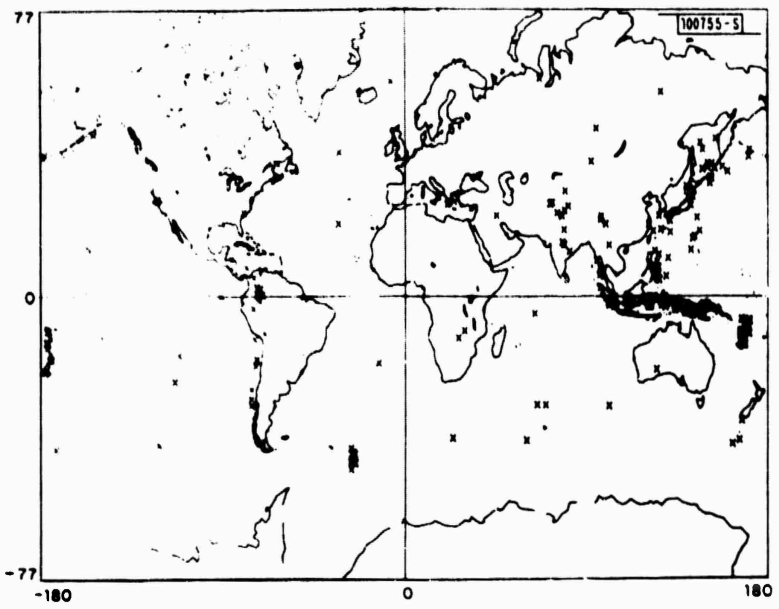

Fig. II-4. Locations of 226 events generated by a synthetic event program (each event is indicated by a cross).

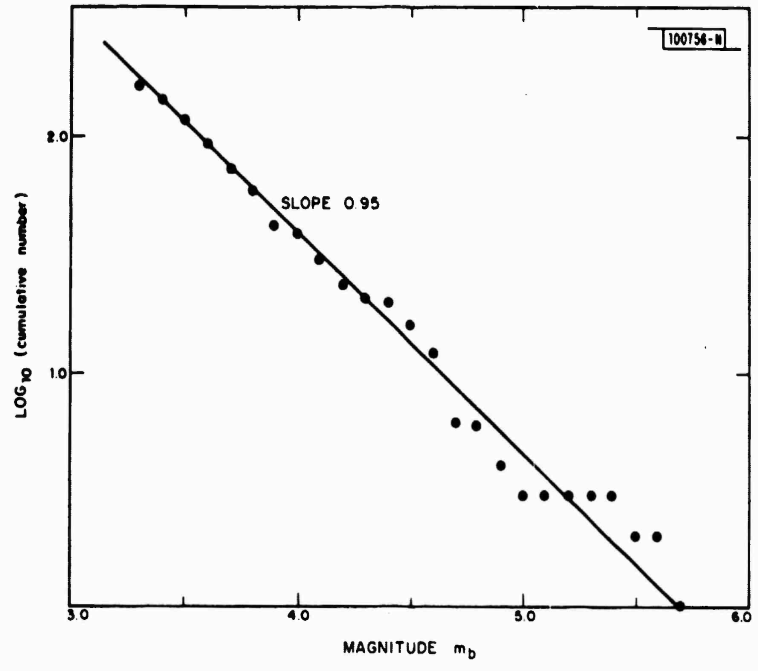

Fig. II-5. Frequency-m_b plot for 226 events shown in Fig. II-4.

III. SEISMIC SOURCE CHARACTERIZATION

ANOMALOUS SURFACE-WAVE RADIATION FROM EASTERN KAZAKH EXPLOSIONS

Some underground explosions produce surface-wave radiation which is radically different from that for others in the same area. Such differences include phase reversal of the Rayleigh waves,[1,2] enhanced Love-wave generation, apparent time delays of the Rayleigh waves by a few seconds,[2,3] and sharp azimuthal dependence of Rayleigh-wave amplitudes.[4] Explanations for these variations include spall closure for the phase reversals and time delays,[2] and "tectonic strain release"[4] for the Love-wave enhancement and Rayleigh azimuthal variation.

We present here a detailed description of differences observed between presumed nuclear explosions within the eastern section of the Eastern Kazakh test area. These events all take place within an extremely restricted region (improved locations for these events are described elsewhere in this report) about 15 km square. We have obtained SRO long- and short-period data for 7 events in this area during 1977-79, whose locations and origin times are given in Table III-1. We have concentrated, in particular, upon the last 3 events, given as numbers 7, 8, and 9 in the table.

TABLE III-1

PRELIMINARY DETERMINATION OF EPICENTER LOCATIONS OF THE EVENTS STUDIED

Event	Date	Time (h:m:s)	Latitude (°N)	Longitude (°N)	m_b
3	08/29/78	02:37:06.3	50.14	78.16	5.60
4	09/15/78	02:36:57.3	49.90	78.93	6.00
5	11/04/78	05:05:58.1	50.02	79.02	5.50
6	11/29/78	04:33:03.6	50.00	78.51	6.20
7	06/23/79	02:56:58.6	49.94	78.97	6.20
8	07/07/79	03:46:58.3	50.06	79.11	5.80
9	08/04/79	03:56:58.0	49.89	78.96	6.00

1. Short-Period Data

The short-period P-waveforms for all the events studied were remarkably similar in both amplitude and waveform shape. Short-period P-waveforms observed at CHTO (Chiengmai, Thailand), MAJO (Matsushiro, Japan), ANMO (Albuquerque, New Mexico), and KAAO (Kabul, Afghanistan) are shown in Fig. III-1 for events 7, 8, and 9. Only very minor differences in shape and amplitude can be seen, and these similarities persisted at other stations and for other events.

2. S-Waves

We also searched for short-period S-waves, but at all stations except KAAO, the detector had switched off and the data were not recorded. No clear short-period S-waves were observed

at Kabul for any of the events available. Long-period S-waves were clearly observed at the closer stations, and were predominantly SV motion. There was no apparent difference in the amount of SV generated from event-to-event.

3. Rayleigh-Wave Amplitudes

Large differences were observed between the amplitudes of the Rayleigh waves generated by event 8 and all the others. Figure III-2(a-c) shows these amplitude differences as observed in the time and frequency domains. The spectral amplitudes have been corrected for geometrical spreading and attenuation of 0.75×10^{-4}/km, to a common distance of 30°; the time-domain amplitudes are directly measured from the data. Excluding event 8, the variation of time- or frequency-domain amplitudes with azimuth is very similar. Event 8 has large amplitudes at stations MAJO, KAAO, and BCAO and small amplitudes at the other stations. Clearly, the source mechanism for this event is radically different from the others.

4. Rayleigh-Wave Phases

In view of the large amplitude differences observed for event 8, which appear to indicate a lobed radiation pattern, we have looked for phase differences between event 8 and the others. Differences in event location become significant here: for example, a difference of 15 km in source-receiver distance corresponds to $\sim\pi/2$ phase shift at the shorter periods (t = 20 sec, C = 3 km/sec, λ = 60 km). It is thus important to (a) obtain the best possible locations and (b) correct the seismograms to be at a common distance for each station. We have used the relative locations obtained for these events as described elsewhere in this report, and corrected the spectral phase for each seismogram so that the event appears to be at a common point chosen to be at the approximate geographical center of the relocated events (50.0°N, 78.90°E). The furthest event from this point (12 km to the southwest) was event 9. We used the dispersion for a shield model[5] to adjust the phase, and the maximum phase delay added (or subtracted) was 0.2 circle. The equalized seismograms were then plotted out for all events recorded at each station. Figure III-3 shows seismograms for events 7, 8, and 9 as recorded at stations KAAO and MAJO, and it can be seen that those for event 8 are in both cases reversed with respect to those for events 7 and 9. This appears to be a reversal only, occurring over the entire frequency range of the data, and no time delay seems to be involved. Similarly clear reversals were observed at some of the other stations, but in some cases the signal amplitudes were so reduced for event 8 that phase changes were hard to determine. We therefore chose to determine phase shifts with respect to event 9 (the largest of the events with a "normal" radiation pattern) in the frequency domain. At each station the cross-correlogram of the seismogram for each event with those for event 8 was computed: its phase is the phase difference of the two seismograms. Table III-2 gives the phase differences determined. In all cases, the seismograms for event 8 were reversed (phase difference of π) with respect to those for event 9. In addition, the seismograms for the other events were apparently similar in phase to event 9; only in a few cases did the phase differences exceed $\pi/5$.

5. Love-Wave Amplitudes and Phases

Figure III-4 shows the maximum Love-wave amplitudes observed on the transverse (after rotation) component seismograms. In all cases, the Love waves were roughly comparable in

TABLE III-2

PHASE DIFFERENCES (MULTIPLES OF π) MEASURED FROM CROSS-CORRELOGRAMS OF EACH SEISMOGRAM WITH THAT FOR EVENT 9 (EXCEPT KONO, NOT OPERATING FOR EVENT 9; EVENT 4 USED)

	Station								
Event	ANMO	ANTO	BCAO	CHTO	GRFO	KAAO	KONO	MAJO	SHIO
3	+0.8	–	–	0.0	–	+0.5	–	–	+0.2
4	0.0	−0.1	–	–	–	−0.2	0.0	−0.1	+0.4
5	−0.3	0.0	–	−0.2	−0.2	+0.5	−0.1	+0.6	0.0
6	−0.1	−0.1	–	−0.1	−0.2	−0.1	−0.1	+0.2	0.0
7	−0.2	−0.5	+0.2	−0.2	–	+0.3	+0.2	0.0	0.0
8	+0.9	+0.9	+0.8	–	+0.8	+0.8	+0.7	+0.8	+0.5
9	0*	0*	0*	0*	0*	0*	–	0*	0*

* By definition.

amplitude with the Rayleigh waves, and the major difference again is for event 8 for which the amplitudes were greater at all azimuths compared with the other events. In addition, there is an apparent radiation pattern for the Love waves which is very similar in pattern to that for the Rayleigh waves, except that the "nodes" of the pattern are not as well pronounced.

We applied the same equalization procedure described above for Rayleigh waves to the Love-wave seismograms, and searched for phase differences between the seismograms for different events. Because of the slightly lower signal-to-noise levels of the Love waves, the results were somewhat less reliable, but no consistent phase differences were observed for any of the events. In particular, no phase reversal was observed for event 8 compared with the others.

6. Conclusions

A careful analysis of SRO data recorded from 7 presumed explosions in a very small area (15 × 20 km) of the Eastern Kazakh test site revealed large differences between an event on 7 July 1979 and all the others. These variations included enhanced Love-wave generation, substantial azimuthal variations in both Love- and Rayleigh-wave amplitudes, and an apparent phase reversal of the Rayleigh waves at all observing azimuths and over the entire period range of 15 to 50 sec studied. However, there is no indication of a time delay of the surface waves, as observed by others.[2,3] No appreciable differences were observed in the short-period P-wave data or in the generation of long-period SV.

These differences clearly indicate a different mechanism for the event of 7 July 1979 as compared with the 5 other events nearby. Possible explanations for these differences, which have been previously observed for other events both in this[2] and other[1,4] areas, include "tectonic stress release" and spall closure. We note here that neither seem particularly attractive explanations: spall closure because there are no apparent differences in the short-period P-waves, and tectonic stress release because several of the "normal" events are within a few

kilometers of the anomalous ones. Later in this report we analyze the Rayleigh-wave radiation in order to interpret these differences in terms of the seismic moment tensor.

R. G. North
M. A. Tiberio

B. RELOCATION OF PRESUMED EXPLOSIONS NEAR THE NUCLEAR TESTING GROUND IN EASTERN KAZAKHSTAN

There are two principal motivations for this work, foremost of which is a need to normalize surface waves from these events to a common focal point (see Sec. A above). The other motivation stems from a desire to investigate systematic errors in locations computed by the usual travel-time analysis. This requires locations, in this case epicenters, that are refined in such a way as to be substantially free of systematic errors, the two prime sources of which are differences between gross earth and regionalized travel-time-distance tables and nonrandom errors in reading arrival times.

Adjustments to a common focus can be represented to a good approximation by $\exp[i\vec{k}(\vec{x} - \vec{x}_c)]$, where $\vec{k}$, $\vec{x}$, and $\vec{x}_c$ are the wave number, location, and common-focus vectors, respectively. To make such adjustments accurately requires locations that are correct to one-fifth to one-tenth of the shortest wave length retained in the spectrum, which for the digital SRO long-period data is about 15 sec or a wave length of about 50 km for fundamental-mode surface waves. Consequently, locations must be accurate to 5 to 10 km. To measure accuracy rather than the precision of the computation, there must be at least one reference event with a known location. Fortunately, such an event occurred near the eastern edge of this testing ground. It is seen as a crater on Landsat imagery.[6] This crater is thought to be the result of an explosion on 15 January 1965. The crater lies at the northern end of a man-made reservoir shown in Fig. III-5.

Accurate epicenters were the result of a two-step process. First, relative epicenters were computed using arrival times of P and PKP phases reported in the Preliminary Determination of Epicenters (PDEs) of the USGS, or times reported in the ISC Bulletins. (We are grateful to Russ Needham for supplying us with recent PDEs prior to publication.) The relative locations were computed by a scheme described in the March 1979 SATS.[7] This scheme is well suited to the situation where distances between events are much less than the shortest ray path, as is the case for this testing ground. The second step involves a constant vector displacement of about 7 km toward the northwest. This displacement places the location of the cratering event (relative to that of the master) at the site of the crater. The resulting epicenters and standard errors are listed in Table III-3.

The master earthquake was chosen arbitrarily from among the better recorded of these presumed explosions. The event of 23 November 1976 is the master. The cratering event was not chosen as the master because it was the least-well-recorded of these events. The number of common stations between the master and the other events ranged from 32 for the cratering event to 136 for the 11 January 1978 event. The closest stations were about 20° away near the southern border of the Soviet Union. Stations internal to the Soviet Union do not report events within their testing grounds. The standard error in the relative location of the cratering event has been added to the standard errors of the other relative locations to yield the error bars shown in Fig. III-5. The standard errors are in every case less than 5 km, which is more than adequate for the normalization of the surface waves to a common focal point.

TABLE III-3
REFINED EPICENTERS

Event	Date	Latitude (°N)	Longitude (°E)
1	6/11/78	49.918 ± 0.026	78.779 ± 0.049
2	7/5/78	49.892 ± 0.029	78.837 ± 0.047
3	8/29/78	50.010 ± 0.043	78.975 ± 0.041
4	9/15/78	49.923 ± 0.028	78.842 ± 0.051
5	11/4/78	50.027 ± 0.039	78.921 ± 0.044
6	11/29/78	49.894 ± 0.041	78.898 ± 0.057
7	6/23/79	49.894 ± 0.032	78.828 ± 0.062
8	7/7/79	50.001 ± 0.047	78.958 ± 0.067
9	8/4/79	49.904 ± 0.034	78.843 ± 0.061
10	10/29/79	49.981 ± 0.039	78.945 ± 0.052
11	11/23/76 (Master)	50.005 ± 0.025	78.937 ± 0.026
12	12/7/76	49.963 ± 0.031	78.814 ± 0.050
13	5/29/77	49.956 ± 0.034	78.729 ± 0.048
14	9/5/77	50.106 ± 0.041	78.914 ± 0.046
15	11/30/77	49.975 ± 0.032	78.854 ± 0.048
Cratering	1/15/65	49.917	79.000

The arrows in the figure point from the PDE location to the refined location. As can be seen, the apparent size of the testing ground has been reduced to a box 20 km in longitude to 15 km in latitude. Excluded from the box is the northernmost event. It seems clear that, even with large sets of arrival times from well-recorded events, locations based on the usual travel-time analysis can be significantly improved by some scheme that is less sensitive to systematic errors in standard time-distance tables and in the reading of arrival times. It should be emphasized that taking arrival-time differences as was done for the relative locations reported here lessens the chance of masking arrival-time errors by a shift in the computed location.

T. J. Fitch
R. G. North

C. MOMENT-TENSOR INVERSION FOR VERY SHALLOW SOURCES

In attempting to invert the surface waves generated by the explosion sources described in the previous section, serious problems emerged which are apparently inherent in moment-tensor analysis of sources at very shallow depths. In particular, the solutions for the full moment tensor were completely dominated by components M_{xz} and M_{yz}. Numerical experiments involving the inversion of synthetic seismograms revealed the reasons for this.

The far-field spectra of Rayleigh $[F_R(h,\omega)]$ and Love $[F_L(h,\omega)]$ waves as given by Mendiguren[8] can be phrased as

$$F_R(h,\omega) = S_R \{A_R [M_{xy} \sin 2\Theta - (M_{yy} - M_{xx}) \cos 2\Theta/2] + C_R M_{zz} + A_R(M_{yy} + M_{xx})/2 - iB_R [M_{yz} \sin\Theta + M_{zx} \cos\Theta]\}$$

$$F_L(h,\omega) = S_L \{A_L [M_{xy} \cos 2\Theta + (M_{yy} - M_{xx}) \sin 2\Theta/2] + iB_L [-M_{yz} \cos\Theta + M_{zx} \sin\Theta]\}$$

where h = source depth, ω = frequency, Θ = azimuth, and (right-hand side notation that of Mendiguren[8])

$$S_R = \frac{y_1^R(0)}{4CUI_1} \left[\frac{2}{\pi kr}\right]^{1/2} \exp[-i(kr - \tfrac{\pi}{4})]$$

$$S_L = \frac{y_1^L(0)}{4CUI_1} \left[\frac{2}{\pi kr}\right]^{1/2} \exp[-i(kr + \tfrac{\pi}{4})]$$

$$A_R = \frac{y_3^R(h)}{C} \quad ; \quad B_R = \frac{y_4^R(h)}{\mu\omega} \quad ; \quad C_R = \frac{y_2^R(h) + \lambda k y_3^R(h)}{\omega(\lambda + 2\mu)}$$

$$A_L = \frac{y_1^L(L)}{C} \quad ; \quad B_L = \frac{y_2^L(h)}{\mu\omega} \quad .$$

A step function is assumed as the source-time function. It can be seen from the above that at any given frequency ω, the relative contribution of any given component of the moment tensor is governed by the associated azimuthal (Θ) variation and the values of A, B, and C. The $y_i^{R/L}$ appearing in the latter are the horizontal (y_1^L, y_1^R) and vertical (y_3^R) displacements, and shear (y_2^L, y_4^R) and normal (y_2^R) stresses obtained by solution of the dispersion equation. A necessary boundary condition of the solution is that the stress components (y_2^L, y_2^R, y_4^R) vanish at the free surface. Thus, at the surface

$$B_R = B_L = 0$$

and, additionally,

$$C_R = \frac{\lambda}{\lambda + 2\mu} A_R \sim \frac{1}{3} A_R \quad .$$

As we go from the surface waves downward, the stress components gradually increase; but at very shallow depths h, such that (h/wavelength) $\ll 1$, the above are approximately true.

We have generated A_R, B_R, and C_R at a variety of depths in a shield model,[9] and these are shown in Fig. III-6 over a period range 6 to 50 sec. At the very shallow depths (0.5 and 1.0 km), B_R is much smaller than either A_R or C_R except at the shorter periods where surface-wave radiation is highly attenuated for teleseismic paths. Thus, any noise whatsoever will be translated into large values of the tensor components M_{xz}, M_{yz} associated with B_R. In addition, since the stress component y_2^R of C_R is very small, C_R has the same variation with frequency as A_R,

making it difficult to separate the azimuthally independent part of $F_R(h, \omega)$. This situation is even more accentuated for the Love-wave variation of A_L, B_L given in Fig. III-7, and reveals the well-known[10] lack of depth resolution provided by Love-wave spectra.

To test the effects of the above features of A_R, B_R, and C_R we have generated synthetic seismograms at a simulated network of 3 stations, designed for good azimuthal coverage, for a source of $M_{xy} = 1.0$ and all other $M_{ij} = 0$, corresponding to a vehicle strike-slip fault, at a variety of source depths. Inversion was carried out in the time domain and the matrix decomposition was carried out in double precision. It became apparent that even numerical noise, corresponding to loss of precision, produces erroneous results at very shallow depths. With actual (rather than synthetic) data, any noise will automatically result in complete dominance of the moment tensor by the dip-slip components of M_{xz} and M_{yz}. In order not to exclude the possibility of such explosive sources, we did not apply the constraint $\Sigma M_{ii} = 0$.

The results, given in Tables III-4 and III-5, are also simply summarized by Fig. III-8 which shows the range of eigenvalues as a function of depth. This can be seen to decrease rapidly from 2×10^4 at 0.5 km to 16 at 10 km depth. Constructing the inverse from the entire set of eigenvalues produced solutions for the seismograms generated for $M_{xy} \neq 0$ only containing large amounts of M_{xz} and M_{yz} at 0.5 km, rapidly decreasing as the source depth was increased. Computed seismograms for the moment tensor thus obtained were compared with the originals and could be exactly overlaid. Seismograms were also computed for a source corresponding to the difference between the input and output moment tensors (mainly M_{xz}, M_{yz}) and these produced reasonable-looking seismograms which were, however, a factor of at least 50 smaller than the input data. Dropping the smaller eigenvalue results in loss of resolution of M_{zz}, which is traded with M_{xx} and M_{yy}. The exact solution (to 4 significant figures) is obtained at all depths only when the 3 largest eigenvalues are retained, but in this case M_{zz} is very poorly resolved, and M_{xz}, M_{yz} essentially unresolved. We conclude that for very shallow sources, only M_{xx}, M_{xy}, and M_{yy} can be adequately resolved. If the constraint $\Sigma M_{zz} = 0$ is applied, as would be appropriate for shallow earthquakes, M_{zz} equals $-(M_{xx} + M_{yy})$ but little can be done about M_{xz} and M_{yz} with the teleseismic pass band.

R. G. North
T. J. Fitch

D. MOMENT-TENSOR INVERSION OF RAYLEIGH WAVES FROM EASTERN KAZAKH EXPLOSIONS

In previous sections we described (1) large differences in surface-wave radiation between presumed explosions in Eastern Kazakh, and (2) fundamental problems in the inversion of surface-wave data from very shallow sources to determine the full moment tensor. We attempt here, subject to the limitations posed by the latter problem, to invert the Rayleigh waves in order to characterize the nature of the source in terms of the resolvable components of the moment tensor.

For an isotropic explosive source, the moment tensor should be characterized by equal diagonal elements ($M_{xx} = M_{yy} = M_{zz}$), and the off-diagonal elements should be zero. The fact that Love waves are virtually always generated by explosions indicates that such a simple description of the source is inadequate. An isotropic explosive source should also produce identical seismograms at all azimuths; this is difficult to determine from data due to our lack of knowledge of propagation corrections, but some explosions do produce what seem to be azimuthally dependent radiation patterns.

TABLE III-4

SOLUTIONS TO SYNTHETIC M_{xy} SEISMOGRAMS*

Source Depth (km)	M_{xx}	M_{xy}	M_{xz}	M_{yy}	M_{yz}	M_{zz}
0.5	0.15	1.0	0.56	0.15	0.35	0.49
1.0	0.027	1.0	0.27	0.027	0.17	0.094
1.5	0.009	1.0	0.17	0.008	0.11	0.032
2.0	0.003	1.0	0.12	0.075	0.075	0.013
3.0	0.0	1.0	0.074	0.046	0.046	0.003
5.0	0.0	1.0	0.036	0.022	0.022	0.003
10.0	0.0	1.0	0.007	0.006	0.006	0.001

* Solution vector obtained by inversion of $M_{xy} = 1.0$, other $M_{ij} = 0$, as a function of depth, when all six eigenvalues are used to construct the inverse.

TABLE III-5

RESOLUTION MATRIX*

M_{xx}	M_{xy}	M_{xz}	M_{yy}	M_{yz}	M_{zz}	
1.0	0.0	0.0	−0.078	0.0	−0.26	M_{xx}
	1.0	0.0	0.0	0.0	0.0	M_{xy}
		0.0	0.0	0.0	0.0	M_{xz}
			0.921	0.0	−0.26	M_{yy}
				0.0	0.0	M_{yz}
					0.16	M_{yy}

* Resolution matrix obtained for 0.5-km depth source when largest 3 eigenvalues only are retained. Note total lack of resolution for M_{xz}, M_{yz} and very poor resolution for M_{zz}, which has considerable trade-off with M_{xx} and M_{yy}.

A major problem in moment-tensor inversion, or any other attempt to characterize the source, is separation of path and source effects. These problems are particularly severe when short-period (up to 50 sec) surface waves are used since these sample mainly the uppermost mantle and crust, where major lateral inhomogeneities exist. At shorter periods (~20 sec), phase and group velocity variations of up to 25 percent are quite common; and attempts to determine attenuation for all but the simplest paths frequently produce such disastrous features as negative Q! It has been pointed out[11] that correct knowledge of the phase velocity, to better than 0.5 percent, is necessary to determine source phase to sufficient accuracy for inversion. To minimize the effects of poor knowledge of path characteristics, we have used a reference event approach somewhat similar to that of Patton.[11]

Ideally, the characteristics of propagation paths from a particular source region should be determined from the surface waves generated by a large event of known moment tensor in that region. The path corrections thus obtained can then be applied to the radiation from smaller events to determine their source moment tensor. The moment tensor of this calibration event can, for example, be estimated from the fault-plane solution for the source if it is large enough to generate the long-period P-waves required. This is not feasible in the present case, as the moderate-size explosions studied were very poor generators of long-period P.

We have thus chosen to invert for the four resolvable components (M_{xx}, M_{yy}, M_{zz}, M_{xy}) of the moment tensor in the following two ways:

(1) Amplitudes only, and

(2) Differences between the seismograms for each event and those for event 9, which we have selected as a calibration event. While we cannot determine the absolute values of phase delay, we earlier determined the phase differences at each station between each event and event 9.

1. Data-Reduction Procedure

The first step here involved correcting some obvious errors in the data. The timing at KAAO (Kabul) was clearly off by exactly 1 min. for late 1978 and early 1979: this was corrected. No anti-alias filter had been applied to the long-period vertical recordings at GRFO: the data were low-pass filtered to make all seismograms comparable in instrument response. Some of the stations are SROs (CHTO, SHIO, ANMO, ANTO, TATO, GRFO, BCAO): the others (MAJO, KAAO, KONO) are ASROs. For uniformity, the seismograms at the ASROs were corrected to appear as if they were recorded on SRO instruments: this involved corrections in the frequency domain for the small differences in amplitude and phase response between the two types of instruments.

For some of the events, there was some interference from other sources: to reduce this and improve signal-to-noise ratios, we determined group-velocity curves for each path from the event with the largest and simplest signals and used these to design a time variable filter. Particular care was taken to ensure that phase differences between events were preserved. The seismograms had all previously been equalized, as described in Sec. A above, to a common focal point of 50.0°N, 78.9°E.

We have chosen to carry out the inversion in the time domain. To construct seismograms containing amplitude information only, we have set the phase delay to be simply $(\frac{\Delta}{c} + \frac{\pi}{2} - \frac{\pi}{4})$ where

$\frac{\Delta}{c}$ is the propagation delay [Δ = distance (km); c = phase velocity] and the $+\frac{\pi}{2}$ and $-\frac{\pi}{4}$ are required to account for, respectively, the assumed step source-time function and the effects of superposition in the frequency domain to construct the seismogram. For the difference in seismograms with respect to those for event 9, we have (a) added an additional phase delay which is the phase difference between the seismogram and that for the same path from event 9, and (b) constructed seismograms which are the difference between these and those for event 9.

2. Inversion

As noted earlier, we carry out inversion in the time domain. This involves, for each set of seismograms for a particular event, calculating 6 synthetic seismograms – one for each component of the moment tensor – and then inverting to determine the optimum linear combination of these which fit the data in a least-squares sense. The linear relation of the moment tensor to the seismogram means that inversion of difference seismograms will yield the difference moment tensor. The synthetic seismograms are computed using the solution at 1 km depth in a shield model. The dispersion for the same model is applied as a path correction to both the data and the synthetics: the choice of model here is not important, since it is canceled in the solution procedure. Since we know that the sources are by definition very shallow, we do not need to include source depth in the inversion procedure. The depth of 1 km used may not be correct, but from Sec. C above we are aware that the excitation parameters A_R and C_R do not change appreciably over the range 0 to 1 km depth and that the most important feature of the solution is that B_R is very small, giving extremely poor resolution for tensor elements M_{xz} and M_{yz}. We are thus able to solve only for the remaining components M_{xx}, M_{yy}, M_{zz}, and M_{xy}, with the additional complications of trade-off between the diagonal elements M_{xx}, M_{yy}, and M_{zz}. The interpretation of such a solution is, of course, extremely limited.

3. Results with Amplitudes Only

The 6 synthetic seismograms corresponding to individual moment-tensor components are computed with the source phase set to zero. The attenuation coefficients used to correct amplitudes are given in Table III-6. Constructing the solution from the 3 largest eigenvalues (those rejected correspond to unresolved M_{xz}, M_{yz}, and poor resolution of M_{zz}), the solutions are shown in Table III-7 for events 4 through 9. The difference between event 8 and the others is immediately apparent from the solution – M_{xy} is much larger, and reversed in sign, for this event compared with the others. If we were able to resolve, and diagonalize the full moment tensor, then the explosive or monopole component would be given by the diagonal elements, and the multipole component by the other elements. The ratio of M_{xy} to the sum of the diagonal elements is also given in Table III-7: it is much larger and reversed in sign for event 8 compared with the others. In the following contributions to this SATS, the problem of separating the multipole components of these incomplete moment tensors is discussed and possible solutions to this problem are proposed. The difference seismograms, with phase differences included, are of particular use in this.

4. Comparison of Predicted and Observed Radiation Patterns

Using the 4 resolved components of the moment tensor, we may compute radiation patterns for comparison with the variation of amplitudes with azimuth described in Sec. A above. In the

TABLE III-6

ATTENUATION COEFFICIENTS USED IN INVERSION

50 to 42 sec	0.5×10^{-4}/km
42 to 36 sec	0.75×10^{-4}/km
36 to 16 sec	1.0×10^{-4}/km

TABLE III-7

MOMENT TENSORS (RESOLVED COMPONENTS ONLY) OBTAINED FOR 6 EVENTS IN EASTERN KAZAKH. UNITS OF 10^{22} dyn-cm.

Event (Date)	M_{xx}	M_{yy}	M_{zz}	M_{xy}	$\frac{M_{xy}}{(M_{xx} + M_{yy} + M_{zz})}$
9 (08/04/79)	5.7	6.0	3.3	−2.8	−0.19
8 (07/07/79)	6.7	8.1	4.2	8.1	+0.43
7 (06/23/79)	4.6	3.6	2.3	−1.6	−0.16
6 (11/29/78)	4.0	2.8	1.9	−0.6	−0.073
5 (11/04/78)	2.0	1.7	1.0	−0.2	−0.048
4 (09/15/78)	3.2	3.7	2.0	−0.6	−0.071

absence of components M_{xz} and M_{yz} we may determine only the real part of the far-field spectrum, given by

$$F_R(\omega) = S_R(\omega)\, A_R(\omega) \left[M_{xy} \sin 2\theta - \frac{(M_{yy} - M_{xx})}{2} \cos 2\theta - \frac{1}{3} M_{zz} + (M_{yy} + M_{xx})/2 \right]$$

for Rayleigh waves, and

$$F_L(\omega) = S_L(\omega)\, A_L(\omega) \left[M_{xy} \cos 2\theta + \frac{(M_{yy} - M_{xx})}{2} \sin 2\theta \right]$$

where the nomenclature is that of Sec. C above and we have assumed $C_R = -1/3\, A_R$ for a very shallow source. Except for the scaling introduced by $S_R(\omega)$, $A_R(\omega)$ and $S_L(\omega)$, $A_L(\omega)$ the radiation patterns obtained are independent of frequency.

The spectral amplitudes calculated at azimuths corresponding to the stations used are shown in Fig. III-9(a-b) for events 7, 8, and 9, and should be compared with the observed variation into azimuth shown in Figs. III-2 and III-4. We have inverted only the Rayleigh waves to determine the moment-tensor components. The match for the Rayleigh waves is good: the similarity of events 7 and 9 is clear, as is the substantial difference between these two and event 8.

The major Love-wave differences observed between events 7, 8, and 9 are (a) the larger amplitude at all azimuths for event 8, and (b) smaller differences between events 7 and 9. These features are well predicted by the moment tensors, as shown in Fig. III-9(b). The large amplitudes observed at KAAO for events 8 and 7 are not, however, predicted. Nevertheless, it is encouraging that the moment tensor determined only from Rayleigh waves predicts the general features of the Love-wave data.

R. G. North
T. J. Fitch

E. TOWARD AN UNDERSTANDING OF THE AZIMUTHALLY DEPENDENT SURFACE-WAVE RADIATION FROM UNDERGROUND EXPLOSIONS

From a previous discussion by North and Fitch (Sec. C above), a useful point-source representation for underground explosions, if it is to be couched in terms of the moment tensor, must be constrained if the data are fundamental mode surface waves. Solutions for the full moment tensor are not realizable because of the poor resolution of the M_{zz} and the dip-slip components M_{xz} and M_{yz} from sources within a few kilometers of the surface. At this writing, a variety of constraints are being tested, with only tentative indications of what may prove to be useful constraints.

Trial-and-error fits to a "faultless" moment tensor using only amplitude data from Eastern Kazakhstan (see Sec. A above) suggest that there is not sufficient information in these data to resolve this moment tensor even if it is constrained to maximize the monopole component. The "faultless" moment tensor in diagonalized form can be written

$$\begin{pmatrix} \lambda & 0 & 0 \\ 0 & \lambda & 0 \\ 0 & 0 & \beta \end{pmatrix} = \begin{pmatrix} a & 0 & 0 \\ 0 & a & 0 \\ 0 & 0 & a \end{pmatrix} + \begin{pmatrix} b/2 & 0 & 0 \\ 0 & b/2 & 0 \\ 0 & 0 & -b \end{pmatrix} ;$$

a and b pertain to the monopole and compensated linear vector dipole (CLVD) components, respectively. If Θ is the polar angle of the major axis of this tensor and ϕ is the azimuth of this axis, the tensor components can be written

$$M_{xx} = \lambda(\cos^2\phi \cos^2\Theta + \sin^2\phi) + \beta \cos^2\phi \sin^2\Theta$$

$$M_{xy} = 1/2 \sin 2\phi(\lambda \cos^2\Theta - \lambda + \beta \sin^2\Theta)$$

$$M_{yy} = \lambda(\sin^2\phi \cos^2\Theta + \cos^2\phi) + \beta \sin^2\phi \sin^2\Theta$$

$$M_{xz} = 1/2 \sin 2\Theta \cos\phi(\beta - \lambda)$$

$$M_{yz} = 1/2 \sin 2\Theta \sin\phi(\beta - \lambda)$$

$$M_{zz} = \lambda \sin^2\Theta + \beta \cos^2\Theta \quad .$$

Because this source representation is axially symmetric when the M_{xz} and M_{yz} terms are not resolvable, there is a 180° ambiguity in the azimuth of the major axis.

If we take M_{xx}, M_{xy}, and M_{yy} as the resolved components of the full moment tensor (see discussion in Sec. D above), then the

$$\tan 2\phi = \frac{M_{xy}}{1/2(M_{xx} - M_{yy})}$$

which leaves us with the problem of solving for λ and β given any two of the knowns and a trial value of Θ. For each trial value of Θ in the range 0° to 180°, the rms of the fit is computed. The results of the Eastern Kazakhstan events revealed a very broad minimum in the rms values centered at a Θ of 90° which corresponds to a horizontal major axis and a maximum in the monopole component. It seems unlikely that a horizontal major axis for the CLVD can represent the actual physical mechanism for each of these underground explosions.

The inclusion of phase information in the data would substantially increase the quality of the data; however, this can not be done at periods of less than 50 sec unless the propagation effect is removed. To remove this effect a reference event (No. 9 in Table III-7) was chosen and spectral phase and amplitude differences were used in inversions for the difference moment tensor. Since events 7, 8, and 9 from Eastern Kazakhstan have nearly the same body-wave magnitude, the difference seismograms should be largely independent of the monopole or simple explosive component of the source functions. However, the interpretation of the difference moment tensors is not simple because the reference event, whichever one might be chosen, does not radiate as a simple monopole. For example, there is always an appreciable Love wave recorded.

The difference moment tensor ΔM_{ij} at a given station is proportional to

$$\left[A(\omega)\, e^{i\delta Q_s} - A^R(\omega)\right] e^{-iQ_s^R}$$

where A and Q refer to amplitude and phase, and the subscript s and superscript R refer to source and reference event, respectively. δQ_s is the phase difference between another event and the reference event at a particular station. Unfortunately, the phase of the reference event by itself Q_s^R has been estimated from the M_{xx}, M_{yy}, and M_{xy} components of the moment-tensor

TABLE III-8

DIFFERENCE MOMENT TENSORS [$\Delta M_{zz} = -(\Delta M_{xx} + \Delta M_{yy})$]*

Event (Date)	ΔM_{xx}	ΔM_{yy}	ΔM_{xy}	ΔM_{xz}	ΔM_{yz}
7 (6/23/79)	0.0009	0.0042	0.0004	−0.0115	−0.0059
8 (7/7/79)	0.0126	0.0137	0.0041	−0.0430	−0.0119

* The condition number for the eigenvalue decomposition was 10^{-2} as in the case of the inversions of phaseless seismograms (see Sec. D above).

solution to the amplitude data from the reference event. It is assumed here that seismograms from all events have been reduced to a common focus.

Table III-8 summarizes the solutions for the moment-tensor differences of events 7 and 8 with respect to event 9. Notice that the zero trace constraint, which is linear, has been used. As in the previously discussed inversions using only amplitudes, the eigenvalues for the dip-slip components ΔM_{xy} and ΔM_{yz} are more than one order of magnitude less than those for the other three components. The dip-slip components are retained because they don't trade off with the others; consequently, you can choose to believe them or not without affecting the interpretation of the three well-resolved components.

A comparison of the ΔM_{xx}, ΔM_{yy}, and ΔM_{xy} with the corresponding components in Table III-7 shows that inversions with and without phase are fundamentally different. With that revelation, it becomes imperative to compute the phase of the reference event in a less arbitrary manner. A scheme involving a joint inversion of all the available data from this testing ground is now being pursued.

T. J. Fitch A. M. Dziewonski
R. G. North J. H. Woodhouse

F. THE SECOND MOMENT TENSOR AND THE LOCATION OF SEISMIC SOURCES

Specific formulas are given for the calculation of theoretical seismograms due to a source of finite spatial and temporal extent, including the terms involving the second spatial and temporal moments. Using these results, expressions are derived for the partial derivatives of synthetic seismograms with respect to source location and time of occurrence, which may be used for the location of earthquakes using complete waveform data. The difference between locations and times so obtained from long-period data, and those obtained conventionally from short-period data can, if sufficiently well determined, give information about the spatial and temporal extent of the source process.

Following Gilbert,[12] Gilbert and Dziewonski,[13] and Backus and Mulcahy,[14] the seismic displacement of a spherically symmetric Earth model due to any seismic source may be written

$$\underset{\sim}{s}(x, t) = \sum_k a_k(t)\, \underset{\sim}{s}_k(x) \qquad \text{(III-1)}$$

with

$$a_k(t) = \int_{V_s} \int_{-\infty}^{t} \left[1 - e^{-\alpha_k(t-t')} \cos \omega_k(t-t')\right] \bar{\underset{\sim}{\varepsilon}}_k(x') : \dot{\underset{\sim}{I}}(\underset{\sim}{x}', t')\, dt'\, d^3x' \quad . \tag{III-2}$$

The notation used here and later will follow, for the most part, that of Gilbert and Dziewonski.[13] The vector fields $\underset{\sim}{s}_k$ are a complete set of eigenfunctions with eigenfrequencies ω_k, and the label k represents the four parameters (q, ℓ, m, n): mode type (toroidal or spheroidal), angular order, azimuthal order, and radial order, respectively. The tensor fields $\underset{\sim}{\varepsilon}_k$ are the elastic strain in the k^{th} mode, and the overbar denotes complex conjugation. The time derivative of the stress glut tensor $\dot{\underset{\sim}{I}}(\underset{\sim}{x}, t)$ completely characterizes the source, and the spatial integration in Eq. (III-2) is over the source region V_s, namely that region in which $\dot{\underset{\sim}{I}}(\underset{\sim}{x}, t)$ is different from zero. The small parameter α_k characterizes the attenuation of the k^{th} mode and is obtainable from perturbation theory for specific models of attenuation in the Earth; terms of first and higher orders in α_k have been neglected in Eq. (III-2) and will be neglected elsewhere.

Backus and Mulcahy[14] have shown that for modes with wavelengths long in comparison with the source dimension, and with periods long in comparison with source duration, Eq. (III-2) may be usefully expanded in terms of the low-order spatial and temporal moments of the glut rate distribution. Specifically, retaining the first two terms in a Taylor expansion of $\bar{\underset{\sim}{\varepsilon}}_k(x') \left[1 - e^{-\alpha_k(t-t')} \times \cos \omega_k(t-t')\right]$ about a fiducial location $\underset{\sim}{x}' = \underset{\sim}{x}_0$ in the source region, and a fiducial time $t' = t_0$ close to the origin time, Eq. (III-2) becomes

$$a_k(t) = \left[1 - e^{-\alpha_k(t-t_0)} \cos \omega_k(t-t_0)\right] \left[M_{ij} \bar{e}_{ij}^{(k)}(\underset{\sim}{x}_0) + \Lambda_{ijp} e_{ij,p}(\underset{\sim}{x}_0)\right]$$

$$- \omega_k e^{-\alpha_k(t-t_0)} \sin \omega_k(t-t_0)\, H_{ij} \bar{e}_{ij}^{(k)}(\underset{\sim}{x}_0) \tag{III-3}$$

at times after the source has ceased to act, where the following glut moments have been defined:

$$M_{ij} = \int_{V_s} \int_{-\infty}^{\infty} \dot{\Gamma}_{ij}(\underset{\sim}{x}, t)\, d^3x\, dt \tag{III-4}$$

$$\Lambda_{ijp} = \int_{V_s} \int_{-\infty}^{\infty} (x_p - x_{0p})\, \dot{\Gamma}_{ij}(\underset{\sim}{x}, t)\, d^3x\, dt \tag{III-5}$$

$$H_{ij} = \int_{V_s} \int_{-\infty}^{\infty} (t - t_0)\, \dot{\Gamma}_{ij}(\underset{\sim}{x}, t)\, d^3x\, dt \quad . \tag{III-6}$$

$\underset{\sim}{M}$ is "the" moment tensor (the sign convention used here is opposite to that of Gilbert and Dziewonski[13]) and $\underset{\sim}{\Lambda}$ and $\underset{\sim}{H}$ describe, in the lowest approximation, the spatial and temporal distributions of the source around the fiducial location $\underset{\sim}{x}_0$ and the fiducial time t_0. Following Backus,[15] we define the centroid location $\underset{\sim}{x}_c$ and the centroid time t_c as the values of $\underset{\sim}{x}_0$, t_0 for which $\underset{\sim}{\Lambda}$ and $\underset{\sim}{H}$ are minimum, in the sense that

$$\Lambda_{ijp}\Lambda_{ijp},\ H_{ij}H_{ij}$$

attain their smallest values. It is readily shown that

$$x_{cp} = x_{0p} + \frac{\Lambda_{ijp} M_{ij}}{M_{rs} M_{rs}} \tag{III-7}$$

$$t_c = t_0 + \frac{H_{ij} M_{ij}}{M_{rs} M_{rs}} \quad . \tag{III-8}$$

The moment tensors $\underset{\sim}{\Lambda}$ and $\underset{\sim}{H}$ relative to this centroid will be denoted by

$$\tilde{\Lambda}_{ijp} = \Lambda_{ijp}(\underset{\sim}{x}_c) \tag{III-9}$$

$$\tilde{H}_{ij} = H_{ij}(t_c) \tag{III-10}$$

and, thus,

$$\Lambda_{ijp}(\underset{\sim}{x}_0) = \tilde{\Lambda}_{ijp} - (x_{0p} - x_{cp})\, M_{ij} \tag{III-11}$$

$$H_{ij}(t_0) = \tilde{H}_{ij} - (t_0 - t_c)\, M_{ij} \quad . \tag{III-12}$$

The tensors $\underset{\sim}{\tilde{\Lambda}}$, $\underset{\sim}{\tilde{H}}$, which satisfy

$$M_{ij} \tilde{\Lambda}_{ijp} = 0 \tag{III-13}$$

$$M_{ij} \tilde{H}_{ij} = 0 \tag{III-14}$$

have the advantage of depending only upon the source, and not on the choice of $\underset{\sim}{x}_0$, t_0.

Equation (III-3) may now be written

$$\begin{aligned} a_k(t) = {} & \left[1 - e^{-\alpha_k (t - t_0)} \cos \omega_k (t - t_0)\right] \\ & \times \{M_{ij} [\bar{e}^{(k)}_{ij}(\underset{\sim}{x}_0) + (x_{cp} - x_{op})\, \bar{e}^{(k)}_{ij,p}(\underset{\sim}{x}_0)] + \tilde{\Lambda}_{ijp}\, \bar{e}^{(k)}_{ij,p}(\underset{\sim}{x}_0)\} \\ & - \omega_k e^{-\alpha_k (t - t_0)} \sin \omega_k (t - t_0) \left[M_{ij} \bar{\bar{e}}^{(k)}_{ij}(\underset{\sim}{x}_0)(t_c - t_0) + \tilde{H}_{ij} \bar{\bar{e}}^{(k)}_{ij}(\underset{\sim}{x}_0)\right] \quad . \end{aligned} \tag{III-15}$$

It is clearly feasible and desirable to obtain constraints upon $\underset{\sim}{\tilde{\Lambda}}, \underset{\sim}{\tilde{H}}$ from long-period data for particular earthquakes; if it is assumed, however, that these contributions are small, Eq. (III-15) leads to a simpler inverse problem for the centroid location $\underset{\sim}{x}_c$ and the centroid time t_c. We have

$$a_k(t) = a_{0k}(t) + (x_{cp} - x_{0p}) \frac{\partial}{\partial x_{0p}} a_{0k}(t) + (t_c - t_0) \frac{\partial}{\partial t_0} a_{0k}(t) \tag{III-16}$$

where

$$a_{0k}(x, t) = \left[1 - e^{-\alpha_k (t - t_0)} \cos \omega_k (t - t_0)\right] \bar{e}_k(\underset{\sim}{x}_0) : \underset{\sim}{M} \quad . \tag{III-17}$$

In order to calculate Eqs. (III-3), (III-15), or (III-16), it is necessary to obtain expressions for $a_k(t)$ in terms of the precomputed scalar eigenfunctions for a particular Earth model. We then have[13]

$$s_r(x, t) = \sum_k a_k(t)\, U_k(r)\, X_\ell^m(0)\, e^{im\phi}$$

$$s_\theta(x,t) = \sum_k a_k(t)\,[V_k(r)\,X_\ell'^m(\theta) + im\,\mathrm{cosec}\,\theta\,W_k(r;X_\ell^m(\theta)]\,e^{im\phi}$$

$$s_\phi(x,t) = \sum_k a_k(t)\,[im\,\mathrm{cosec}\,\theta\,V_k(r)\,X_\ell^m(\theta) - W_k(r)\,X_\ell'^m(\theta)]\,e^{im\phi} \qquad \text{(III-18)}$$

where the notation follows that of Gilbert and Dziewonski.[13]

We denote by f_i the six independent elements of the moment tensor:[13]

$$f_1 = M_{rr}\ ,\quad f_2 = M_{\theta\theta}\ ,\quad f_3 = M_{\phi\phi}\ ,$$

$$f_4 = M_{r\theta}\ ,\quad f_5 = M_{r\phi}\ ,\quad f_6 = M_{\theta\phi}$$

and by ϵ_i the corresponding elements of strain at the source (the mode index k is suppressed)

$$\epsilon_1 = e_{rr}\ ,\quad \epsilon_2 = e_{\theta\theta}\ ,\quad \epsilon_3 = e_{\phi\phi}\ ,$$

$$\epsilon_4 = 2e_{r\theta}\ ,\quad \epsilon_5 = 2e_{r\phi}\ ,\quad \epsilon_6 = 2e_{\theta\phi}\ . \qquad \text{(III-19)}$$

Similarly, we shall denote by λ_i, e_i the 18 independent elements of $\underset{\sim}{\Lambda}, \underset{\sim}{\underset{\sim}{\nabla e}}$:

$$\lambda_1 = \Lambda_{rrr}\ ,\quad \lambda_2 = \Lambda_{\theta\theta r}\ ,\quad \lambda_3 = \Lambda_{\phi\phi r}\ ,\quad \lambda_4 = \Lambda_{r\theta r}\ ,\quad \lambda_5 = \Lambda_{\phi r}\ ,$$

$$\lambda_6 = \Lambda_{\theta\phi r}\ ,\quad \lambda_7 = \Lambda_{rr\theta}\ ,\quad \lambda_8 = \Lambda_{\theta\theta\theta}\ ,\quad \lambda_9 = \Lambda_{\phi\phi\theta}\ ,$$

$$\lambda_{10} = \Lambda_{r\theta\theta}\ ,\quad \lambda_{11} = \Lambda_{r\phi\theta}\ ,\quad \lambda_{12} = \Lambda_{\theta\phi\theta}\ ,\quad \lambda_{13} = \Lambda_{rr\phi}\ ,$$

$$\lambda_{14} = \Lambda_{\theta\theta\phi}\ ,\quad \lambda_{15} = \Lambda_{\phi\phi\phi}\ ,\quad \lambda_{16} = \Lambda_{r\theta\phi}\ ,\quad \lambda_{17} = \Lambda_{r\phi\phi}\ ,$$

$$\lambda_{18} = \Lambda_{\theta\phi\phi}\ . \qquad \text{(III-20)}$$

$$e_1 = e_{rr;r}\ ,\quad e_2 = e_{\theta\theta;r}\ ,\quad e_3 = e_{\phi\phi;r}\ ,\quad e_4 = 2e_{r\theta;r}\ ,\quad e_5 = 2e_{r\phi;r}\ ,$$

$$e_6 = 2e_{\theta\phi;r}\ ,\quad e_7 = e_{rr;\theta}\ ,\quad e_8 = e_{\theta\theta;\theta}\ ,\quad e_9 = e_{\phi\phi;\theta}\ ,$$

$$e_{10} = 2e_{r\theta;\theta}\ ,\quad e_{11} = 2e_{r\phi;\theta}\ ,\quad e_{12} = 2e_{\theta\phi;\theta}\ ,\quad e_{13} = e_{rr;\phi}\ ,$$

$$e_{14} = e_{\theta\theta;\phi}\ ,\quad e_{15} = e_{\phi\phi;\phi}\ ,\quad e_{16} = 2e_{r\theta;\phi}\ ,\quad e_{17} = 2e_{r\phi;\phi}\ ,$$

$$e_{18} = 2e_{\theta\phi;\phi} \qquad \text{(III-21)}$$

where a semicolon is used to denote the appropriate spherical component of the Cartesian third-rank tensor $e_{ij,k}$. Similarly, we shall write

$$h_1 = H_{rr}\ ,\quad h_2 = H_{\theta\theta}\ ,\quad h_3 = H_{\phi\phi}\ ,\quad h_4 = H_{r\theta}\ ,\quad h_5 = H_{r\phi}\ ,\quad h_6 = H_{\theta\phi}$$

for the elements of the time moment tensor H. Equation (III-3) may now be written

$$a_k(t) = \left[1 - e^{-\alpha_k(t-t_0)}\cos\omega_k(t-t_0)\right](\underset{\sim}{f}\cdot\bar{\underset{\sim}{\epsilon}} + \underset{\sim}{\lambda}\cdot\bar{\underset{\sim}{e}})$$

$$-\omega_k e^{-\alpha_k(t-t_0)}\sin\omega_k(t-t_0)\,\underset{\sim}{h}\cdot\bar{\underset{\sim}{\epsilon}}\ . \qquad \text{(III-22)}$$

TABLE III-9

PARAMETERS FOR THE EXCITATION DUE TO FIRST- AND SECOND-MOMENT TENSORS

	Spheroidal Modes				Toroidal Modes			
	m = 0	m = ±1	m = ±2	m = ±3	m = 0	m = ±1	m = ±2	m = ±3
$\bar{\epsilon}_1$	$k_0\dot{U}$							
$\bar{\epsilon}_2$	$1/2\,k_0F$		$k_2r^{-1}V$				$\mp ik_2r^{-1}W$	
$\bar{\epsilon}_3$	$1/2\,k_0F$		$-k_2r^{-1}V$				$\pm ik_2r^{-1}W$	
$\bar{\epsilon}_4$		$-k_1E_S$				$\pm ik_1E_T$		
$\bar{\epsilon}_5$		$\pm ik_1E_S$				E_Tk_1		
$\bar{\epsilon}_6$			$\mp 2ik_2r^{-1}V$				$-2k_2r^{-1}W$	
$\bar{e}_1$	$k_0\ddot{U}$							
$\bar{e}_2$	$-k_0P_5$		k_2P_4				$\pm ik_2q_1$	
$\bar{e}_3$	$-k_0P_5$		$-k_2P_4$				$\mp ik_2q_1$	
$\bar{e}_4$		$-k_1(\ddot{V} + p_1)$				$\pm ik_1(\ddot{W} + q_1)$		
$\bar{e}_5$		$\pm ik_1(\ddot{V} + p_1)$				$k_1(\ddot{W} + q_1)$		
$\bar{e}_6$			$\mp 2ik_2P_4$				$2k_2q_1$	
$\bar{e}_7$		$-k_1P_1$				$\pm ik_1q_1$		
$\bar{e}_8$		$k_1(p_6 + p_7)$		$-k_3r^{-2}V$		$\mp ik_1(q_6 + q_7)$		$\pm ik_3r^{-2}W$
$\bar{e}_9$		k_1p_7		$k_3r^{-2}V$		$\mp ik_1q_7$		$\mp ik_3r^{-2}W$
$\bar{e}_{10}$	$k_0(p_3 - p_5)$		$k_2(p_2 + p_4)$				$\mp ik_2(q_2 - q_1)$	
$\bar{e}_{11}$			$\mp ik_2(p_2 + p_4)$		k_0q_5		$-k_2(q_2 - q_1)$	
$\bar{e}_{12}$		$\mp ik_1p_6$		$\pm 2ik_3r^{-2}V$		$-k_1q_6$		$2k_3r^{-2}W$
$\bar{e}_{13}$		$\pm ik_1p_1$				k_1q_1		
$\bar{e}_{14}$		$\mp ik_1p_7$		$\pm ik_3r^{-2}V$		$-k_1q_7$		$k_3r^{-2}W$
$\bar{e}_{15}$		$\mp ik_1(p_6 + p_7)$		$\mp ik_3r^{-2}V$		$-k_1(q_6 + q_7)$		$-k_3r^{-2}W$
$\bar{e}_{16}$			$\mp ik_2(p_2 + p_4)$		$-k_0q_5$		$-k_2(q_2 - q_1)$	
$\bar{e}_{17}$	$k_0(p_3 - p_5)$		$-k_2(p_2 + p_4)$				$\pm ik_2(q_2 - q_1)$	
$\bar{e}_{18}$		k_1p_6		$2k_3r^{-2}V$		$\mp ik_1q_6$		$\mp 2ik_3r^{-2}W$

Specific forms for $\bar{e}_i$ are given by Gilbert and Dziewonski[13] and are repeated in Table III-9. Forms for e_i also are listed in Table III-9, and the notation is given in Table III-10. The partial derivatives with respect to source location and time of occurrence in Eq. (III-16) are

$$\frac{\partial a_{0k}}{\partial r_0} = \left[1 - e^{-\alpha_k (t-t_0)} \cos \omega_k (t - t_0)\right] \left(\sum_{i=1}^{6} f_i \bar{e}_i \right)$$

$$\frac{1}{r_0} \cdot \frac{\partial a_{0k}}{\partial \theta_0} = \left[1 - e^{-\alpha_k (t-t_0)} \cos \omega_k (t - t_0)\right] \left(\sum_{i=1}^{6} t_i \bar{e}_{i+6} \right)$$

TABLE III-10

NOTATIONS USED IN TABLE III-9

Spheroidal Modes	Toroidal Modes
$F = r^{-1}[2U - \ell(\ell+1)V]$	
$E_S = \dot{V} - r^{-1}(V - U)$	$E_T = \dot{W} - r^{-1}W$
$p_1 = r^{-1}(\dot{U} - \dot{V} - r^{-1}U + r^{-1}V)$	$q_1 = -r^{-1}(\dot{W} - r^{-1}W)$
$p_2 = r^{-2}(U - 2V)$	$q_2 = -2r^{-2}W$
$p_3 = r^{-1}[\dot{U} - r^{-1}U + 1/2\, r^{-1}\ell(\ell+1)(2V - U)]$	
$p_4 = r^{-1}(\dot{V} - r^{-1}V)$	
$p_5 = r^{-1}[1/2\ell(\ell+1)(\dot{V} - r^{-1}V) - \dot{U} + r^{-1}U]$	$q_5 = 1/2\, r^{-1}\ell(\ell+1)(\dot{W} - r^{-1}W)$
$p_6 = r^{-1}[1/2 r^{-1}\ell(\ell+1)V - \dot{V} - r^{-1}U]$	$q_6 = r^{-1}[1/2\, r^{-1}\ell(\ell+1)W - \dot{W}]$
$p_7 = -r^{-2}\{1/4[\ell(\ell+1) - 2]V + rF\}$	$q_7 = -1/4 r^{-2}[\ell(\ell+1) - 2]W$

U, V, W to be evaluated at radius $r = |\underline{x}_0|$

$$k_n = \frac{1}{2^n}\left(\frac{2\ell+1}{4\pi} \cdot \frac{(\ell+n)!}{(\ell-n)!}\right)^{1/2}$$

i.e., $k_0 = \left(\frac{2\ell+1}{4\pi}\right)^{1/2}$; $k_n = 1/2\,[(\ell+n)(\ell-n+1)]^{1/2} k_{n-1}$

$$\frac{1}{r_0 \sin\theta_0} \cdot \frac{\partial a_{0k}}{\partial \phi_0} = \left[1 - e^{-\alpha_k (t-t_0)} \cos\omega_k (t - t_0)\right]\left(\sum_{i=1}^{6} f_i \bar{e}_{i+12}\right)$$

$$\frac{\partial a_{0k}}{\partial t_0} = -\omega_k e^{-\alpha_k (t-t_0)} \sin\omega_k (t - t_0)\left(\sum_{i=1}^{6} f_i \bar{c}_i\right)$$

where (r_0, θ_0, ϕ_0) are the spherical coordinates of the source location $\underset{\sim}{x}_0$.

Discussion

Detailed formulas have been given for the formulation of the linear inverse problem for moments up to the second, and/or for the linearized inverse problem of source location using complete waveform data. The problem of simultaneously determining the source moment tensor $\underset{\sim}{M}$ and the centroid location and time is not linearizable and must proceed by iterations (see Sec. G below) in which the moment tensor and source location are alternately fixed, and where the process is found to be rapidly convergent.

It may be remarked that it is only in the limit of long periods and wavelengths that the true centroid location and time will, even theoretically, be obtained. In general, for a finite number of records and a finite frequency band, a location will result which depends upon frequency and station distribution. Nevertheless, it is to be expected that for relatively small sources the answer will be close to the centroid, and in any case will give a valuable measure of the size and duration of the source when compared with conventionally determined locations and origin times, provided, of course, that these are determined with sufficient accuracy. If the process could be carried out in a number of different frequency bands, the resulting locations and times, as a function of frequency, would be very interesting data for the study of sources.

J. H. Woodhouse

G. INVERSION OF SRO AND ASRO SEISMOGRAMS FOR THE MECHANISM AND LOCATION OF THE SOURCE

This report describes application of a novel procedure: simultaneous inversion of the waveform data for the equivalent system of forces at the source and the hypocentral parameters. Usually, location of an earthquake and estimation of source mechanism are performed separately. Inversion for the moment tensor is made assuming that the hypocentral parameters are known. This may not always be a correct assumption; for sources of finite size, the best point-source location need not be coincident with the hypocenter determined from the arrival times of short-period body waves.

The approach presented here stems from earlier work of Dziewonski,[16] who outlined an efficient procedure for evaluation of the elements of the moment tensor by inversion of entire wavetrains consisting of long-period body waves. A very significant development has been derivation by Woodhouse (see Sec. F above) of the coefficients for perturbation of excitation parameters due to changes in the hypocentral parameters of the source and in the origin time.

We feel that our approach has significant potential for research in seismology. In addition to providing very stable, routine determinations of moment tensor for earthquakes in a range of body-wave magnitudes from 5.5 to 7.0, differences between the standard hypocentral locations

and locations of the centroids of the stress glut could lead to reliable estimates of temporal and spatial dimension of the source region.

It is also possible that the standard locations are in error; we are poorly protected against absolute errors in hypocentral location if lateral heterogeneity is not known. It may be expected that, by using signals of wavelengths more than an order-of-magnitude greater, this effect could be detected.

Another aspect of the proposed method is its high resolution for the source depth. Because we are analyzing entire wavetrains of body waves, the energy radiated upward and reflected from the surface is, on average, equal to the downward radiated energy; thus, we include the complete suite of the "depth phases" in our analysis.

The process described here requires determination of a starting solution for the moment tensor using hypocentral parameters furnished by the National Earthquake Information Service, for example. This part of the procedure is directly related to the approach of Gilbert and Dziewonski.[13]

$$u_k(\Delta, \phi, t) = \sum_{i=1}^{6} A_{ik}^{0}(\Delta, \phi, r_s, t) \cdot M_i^0 \qquad \text{(III-23)}$$

where u_k is the k^{th} record in the set of seismograms to be inverted, $A_{ik}(\Delta, \phi, r_s, t)$ is the synthetic seismogram associated with the i^{th} component of the unit moment tensor, and M_i are the elements of the moment tensor (indices from 1 through 6 are assigned to M_{rr}, $M_{\theta\theta}$, $M_{\phi\phi}$, $M_{r\theta}$, $M_{r\phi}$, and $M_{\theta\phi}$, respectively). A_{ik} are obtained by summation of normal modes; the superscript denotes the zeroth (starting) iteration.

In practice, we use the data from SRO and ASRO stations. Theoretical seismograms are obtained using the normal-mode catalog computed by Buland[17] for an Earth model 1066B of Gilbert and Dziewonski.[13] Since this catalog does not extend to periods below 45 sec, we apply a $\cos^2$ taper to the spectra of observed and theoretical seismograms in the period range from 45 to 60 sec, in order to avoid the ringing associated with an abrupt truncation. Because of the response of the instruments used, this leads to a rather narrow-band signal with the maximum energy at about 55 sec.

The signals used span the time from the arrival of the P-wave until the arrival of the fundamental-mode surface waves: Rayleigh, for the vertical and longitudinal components; Love, for the transverse component. An average Earth model would not be useful in the analysis of surface waves as, in the period range considered here, their dispersion and amplitudes are too much perturbed by lateral heterogeneity.

The segments of records with obvious glitches are eliminated, and a preliminary inversion is performed to examine the data for consistency; this allows us to discover, for example, reversed polarities of components and erroneous multiplexing. After these corrections are made, the data are inverted again to obtain the starting solution: M_i^0.

At this stage the inverse problem is expanded to allow for perturbations in the source radius r_s, source co-latitude θ_s, and longitude λ_s, as well as the origin time t_0. For the j^{th} iteration, the equations of condition associated with the k^{th} recording are:

$$u_k(t) - A_{ki}^{(j-1)} \cdot (t)\, M_i^{(j-1)} = A_{ki}^{(j-1)}(t)\, \delta M_i + b_k(t)\, \delta r_s + c_k(t)\, \delta\theta_s + d_k(t)\, \delta\lambda_s + e_k(t)\, \delta t_0 \quad ; \qquad \text{(III-24)}$$

TABLE III-11

SIMULTANEOUS SOLUTIONS FOR MOMENT TENSOR AND LOCATION

Date	PDE (Monthly Listing)				Our Results				Scale Factor	Principal Axes of Moment Tensor					
	Origin Time	Coordinates		Depth	δt_o	$\delta\theta_s$	$\delta\lambda_s$	δh_s		Tension Axis		"Null" Axis		Compression Axis	
	(h:m:s)	Latitude	Longitude	(km)	(sec)	(deg)	(deg)	(km)	(dyn-cm)	Value	Plunge/Az	Value	Plunge/Az	Value	Plunge/Az
03/07/78	2:48:47.6	32.01°N	137.61°E	439	7.7	0.49	−0.62	−19	10^{26}	3.9	52/66	0.2	0/157	−4.1	37/247
03/15/78	22:4:40.1	26.42°N	140.56°E	263	3.5	0.08	0.32	−5	10^{25}	4.7	13/65	1.3	59/178	−6.0	28/329
09/06/78	11:7:43.1	13.32°S	167.14°E	198	9.3	−0.01	−0.46	−8	10^{26}	1.6	64/127	0.0	24/333	−1.6	11/239
09/15/78	11:39:25.1	48.25°N	154.28°E	44	2.6	0.53	1.49	−14	10^{25}	1.1	84/286	0.0	1/27	−1.1	6/117
09/23/78	16:32:11.1	13.92°S	167.21°E	201	9.4	0.02	−0.31	−1	10^{26}	1.4	79/154	0.0	11/333	−1.4	0/248
10/01/78	13:23:50.1	6.68°N	123.98°E	46	3.0	−0.03	0.45	−31	10^{24}	5.4	74/76	0.0	0/167	−5.4	15/257
12/18/78	10:15:53.1	54.48°S	2.07°E	10	8.2	0.32	0.56	0	10^{26}	1.4	3/179	0.0	77/281	−1.4	13/88
04/24/79	1:45:10.0	20.84°S	178.64°W	599	3.2	−0.05	−0.03	1	10^{25}	2.1	23/168	0.4	5/76	−2.5	66/334

with the implied summation over i (i = 1, 2, . . . , 6), and where

$$b_k(t) = \partial/\partial r \, [A_{ki}^{(j-1)}(t)]_{r=r_s} \, M_i^{(j-1)} \quad ;$$

$$c_k(t) = \partial/\partial\theta \, [A_{ki}^{(j-1)}(t)]_{\theta=\theta_s} \, M_i^{(j-1)} \quad ;$$

$$d_k(t) = \sin\theta_s \, \partial/\partial\lambda \, [A_{ki}^{(j-1)}(t)]_{\lambda=\lambda_s} \, M_i^{(j-1)} \quad ;$$

$$e_k(t) = \partial/\partial t \, [A_{ki}^{(j-1)}(t)] \, M_i^{(j-1)} \quad .$$

Coefficients needed to evaluate the kernel functions b, c, d, and e are given in Sec. F above. Equivalent expressions could also be derived by the appropriate differentiation of Eqs. (2.2.30) and (2.2.31) of Gilbert and Dziewonski.[13] The inverse problem is usually solved in the frequency domain.

Our experience shows that the process converges rapidly; almost without exception, no substantial decrease in the rms error or change in the solution is encountered after third iteration, even if the horizontal shift of the source was as large as 140 km, encountered in the case of the Bouvet Island earthquake of 18 December 1978.

Numerical results of our analysis of eight earthquakes ranging in depth from 10 to 600 km and in seismic moment from 5×10^{24} to 4×10^{26} dyn-cm are listed in Table III-11. We compare the locations obtained from the standard methods. Typically, data from 12 to 14 stations were used in the analysis.

The resulting moment tensors are represented here in terms of the moments and directions of the principal axes (tension is positive, compression is negative). The solutions have been constrained to have a vanishing trace of the tensor ($M_{rr} + M_{\theta\theta} + M_{\phi\phi} = 0$); in our experiments we have found no evidence that the isotropic component is necessary to satisfy the data. This does not mean that this component is not present; our data are so clearly dominated by the shear energy that, at least in this stage of the experiment, attempts to recover the monopole component of the source do not seem warranted.

It was not required, however, that the source should be of the double-couple type. Yet, in six out of eight solutions and for all shallow sources, one of the eigenvalues is, for practical purposes, zero. This means that the data demand that the source be a double couple. It is also of interest to note that the intermediate eigenvalue ("null" axis, for a double-couple solution) generally decreased as a result of iteration for the hypocentral location. This may mean that bias in moment-tensor solutions could be introduced by using the standard locations or by lateral heterogeneities.

In the remaining two cases, for which the intermediate eigenvalue is nonzero, there is some evidence that measurable improvement in fitting synthetics to the data can be accomplished by introducing nonzero stress along all principal axes of the moment tensor. Clearly, many more deep and intermediate events should be analyzed in order to determine whether such stress patterns are consistent and statistically significant. It is an issue of substantial importance to our understanding of the nature of earthquakes at depths at which brittle fracture is not likely.

Figure III-10 shows the distribution of stations used to analyze a 600-km-deep shock under the Fiji Islands. As for most of the earthquakes in the circum-Pacific belt, the azimuthal distribution of stations is not well balanced: 9 out of 14 stations are in a single azimuthal quadrant.

Addition of the planned digital WWSSN stations would significantly contribute to an improved azimuthal coverage. The hypocentral parameters of the event of 24 April 1979 changed very little: roughly 5 km in location and +3.2 sec in origin time. In Figs. III-11(a) and (b) we compare the observed seismograms with the synthetics. In most cases, the fit is very good. We wish to draw attention to the traces of the vertical component of station KONO; the analyzed part of the recording, delineated by broken vertical lines, is 45 min. long, and the synthetics reproduce the observed record in all important details. The same is true in respect to nearly all vertical and transverse components, agreement for SNZO, NWAO, and ANMO (transverse component) is spectacular. However, the synthetics for longitudinal components predict wavetrains that, at late times, have systematically lower amplitudes. This cannot be explained by an error in source mechanism or the Q-structure of the model, since we would not then expect a satisfactory agreement for vertical and transverse components. We think that the explanation must be related to differences between the elastic parameters of the upper mantle in the real Earth and in the model 1066B. The effect is clearly a noticeable one; it is possible to think that studies such as this one will lead to the refinement of the Earth structure in addition to contributing to our knowledge of global seismicity.

Figures III-12(a) and (b) shows selected seismograms and synthetics for an intermediate-depth shock of 23 September 1978. The epicenter is not too distant from that discussed before and, consequently, station coverage is very similar to that shown in Fig. III-10. The change in epicentral coordinates is much greater in this case; depth decreased by 8 km and, although the latitude remained the same, longitude decreased by 0.46°; also, the origin time increased by 9.3 sec. If this difference is not an artifact of lateral heterogeneities (the fact that the location of the 24 April 1979 event remained unchanged would tend to indicate that this is not the case) or poor standard location, then one would have to infer that this earthquake of seismic moment 1.6×10^{26} dyn-cm had substantial source dimensions (~100 km) and a duration of roughly 20 sec.

Comparison of observed seismograms with the synthetics gives an opportunity to appreciate path dependence of the quality of fit. Most of the stations fit well; an important exception is represented by stations MAIO and KAAO; the paths are very similar for these two stations and they cross the most tectonically disturbed region of Asia. Although the observed and synthetic seismograms show good agreement for early phases (traveling through the lower mantle), the multiply reflected S_V waves show substantial differences; about 35 min. after the origin time the synthetics are 180° out of phase with respect to observations for the vertical and longitudinal components. It is interesting to note that the effect on S_H waves is much less; here the agreement is rather good throughout. Observations at CHTO, closer to the epicenter but only 10° different in azimuth at the source, are in excellent agreement with the synthetics, confirming the evidence for anomalous properties of the remainder of the path.

Each of the eight analyses brought to light some new and unexpected, at least by us, information. Because of the format of this report, we cannot provide a detailed description of the results. We feel that the approach outlined here can be efficiently used to learn more about the earthquakes and the Earth.

Teh-An Chou*
A. M. Dziewonski

* Department of Geological Sciences, Harvard University.

REFERENCES

1. Seismic Discrimination Semiannual Technical Summary, Lincoln Laboratory, M.I.T. (30 December 1970), DDC AD-718971.

2. E. Rygg, "Anomalous Surface Waves from Underground Explosions," Bull. Seismol. Soc. Am. 69, 1995-2002 (1979).

3. D. von Seggern, "Seismic Surface Waves from Amchitka Island Test Site Events and Their Relocation to Source Mechanism," J. Geophys. Res. 78, 2467-2474 (1973).

4. M. N. Toksoz, A. Ben-Menahen, and D. G. Harkrider, "Determination of Source Parameters of Explosions and Earthquakes by Amplitude Equalization of Seismic Surface Waves: I. Underground Nuclear Explosions," J. Geophys. Res. 69, 4344-4366 (1964).

5. D. G. Harkrider, "Surface Waves in Multilayered Elastic Media: II. Higher Mode Spectra and Spectral Ratios from Point Sources in Layered Media," Bull. Seismol. Soc. Am. 60, 1937-1988 (1970).

6. H. C. Rodean, " ISC Events from 1964 to 1976 at and Near the Nuclear Testing Ground in Eastern Kazakhstan," Lawrence Livermore Laboratory Report, UCRL 52856 (1979).

7. Seismic Discrimination Semiannual Technical Summary, Lincoln Laboratory, M.I.T. (31 March 1979), DDC AD-A073772/6.

8. J. A. Mendiguren, "Inversion of Surface Wave Data in Source Mechanism Studies," J. Geophys. Res. 82, 889-894 (1977).

9. D. G. Harkrider, "Surface Waves in Multilayered Elastic Media. II. Higher Mode Spectra and Spectral Ratios from Point Sources in Layered Media," Bull. Seismol. Soc. Am. 60, 1937-1988 (1970).

10. Y. B. Tsai and K. Aki, "Precise Focal Depth Determination from Amplitude Spectra of Surface Waves," J. Geophys. Res. 75, 5729-5743 (1970).

11. H. Patton, "Reference Point Equalization Method for Determining the Source and Path Effects of Surface Waves," J. Geophys. Res. 85, 821-848 (1980).

12. F. Gilbert, "Excitation of the Normal Modes of the Earth by Earthquake Sources," Geophys J R. Astr. Soc. 22. 223-226 (1971).

13. F. Gilbert and A. M. Dziewonski, "An Application of Normal Mode Theory to the Retrieval of Structural Parameters and Source Mechanisms from Seismic Spectra," Phil. Trans. Roy. Soc. London A278, 187-269 (1975).

14. G. E. Backus and M. Mulcahy, "Moment Tensors and Other Phenomenological Descriptions of Seismic Sources – I. Continuous Displacements," Geophys. J. R. Astr. Soc. 46, 341-361 (1976).

15. G. E. Backus, "Interpreting the Seismic Glut Moments of Total Degree Two or Less," Geophys. J. R. Astr. Soc. 51, 1-25 (1977).

16. A. M. Dziewonski, "Rapid Computation of Synthetic Seismograms by Superposition of Normal Modes," EOS, Trans. Am. Geophys. Un. 59, 325 (1978).

17. R. P. Buland, "Retrieving the Seismic Moment Tensor," Ph.D. Thesis, University of California, San Diego (1976).

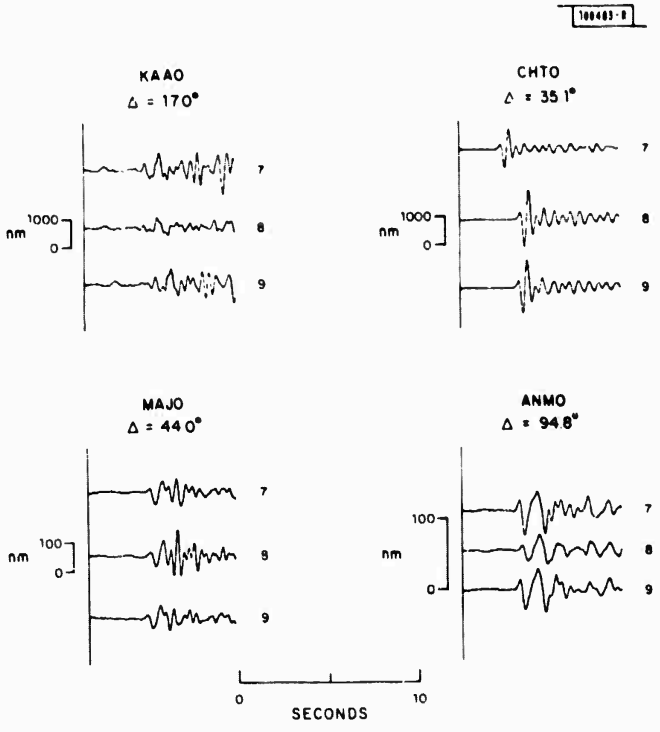

Fig. III-1. Short-period waveforms observed at four SRO/ASRO stations from events 7, 8, and 9 (see Table III-1).

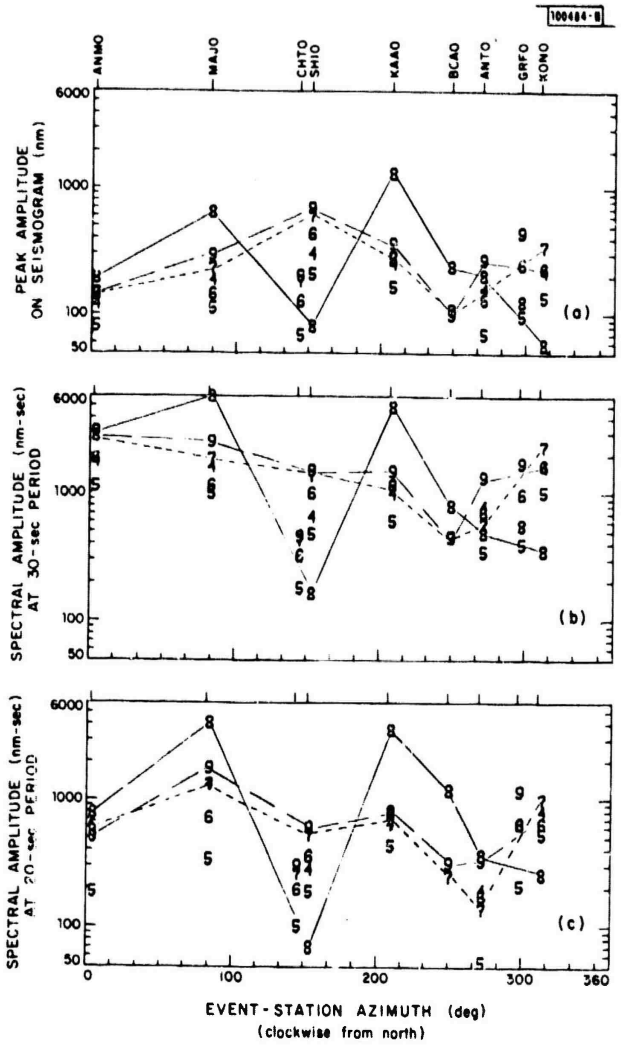

Fig. III-2. Rayleigh-wave amplitudes as a function of azimuth: (a) peak amplitude on seismogram; (b) 30-sec period spectral amplitudes, corrected for geometrical spreading and attenuation of 0.75×10^4/km; and (c) same as (b) but 20-sec period.

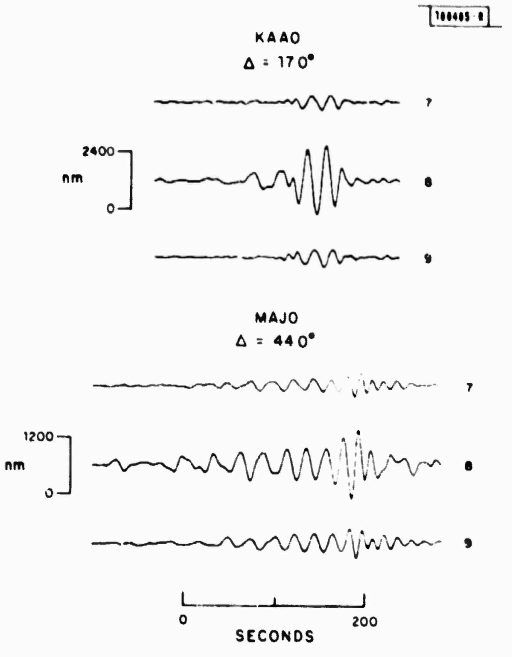

Fig. III-3. Rayleigh-wave seismograms for events 7, 8, and 9 at KAAO (Kabul) and MAJO (Matsushiro) showing phase reversal of seismograms for event 8.

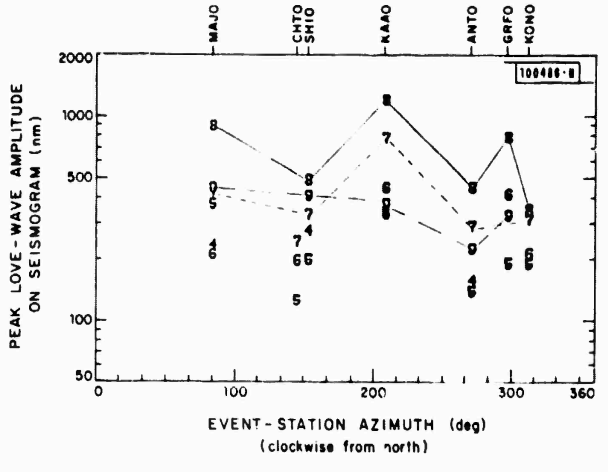

Fig. III-4. Peak Love-wave amplitudes as a function of azimuth, measured from seismograms.

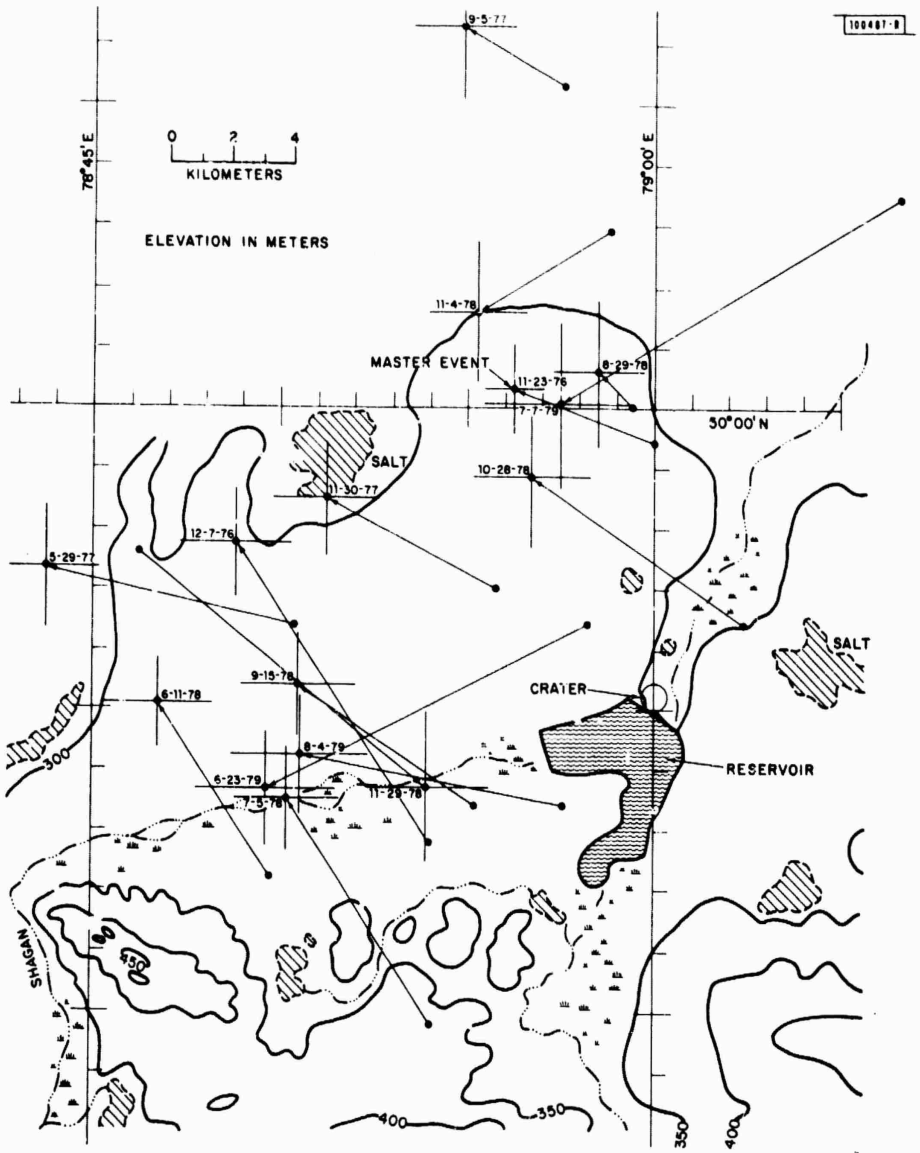

Fig. III-5. Event locations and geographical features near nuclear testing ground in Eastern Kazakhstan.

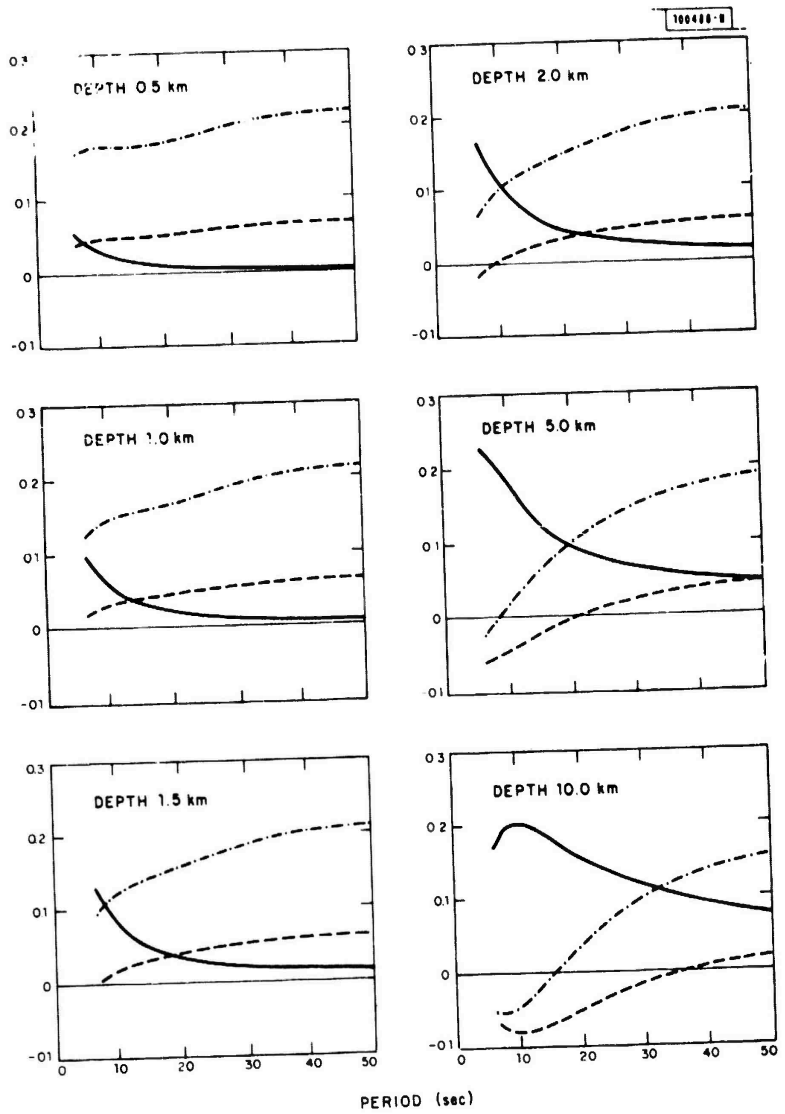

Fig. III-6. Values of A_R, B_R, and C_R (see text) over period range 6 to 50 sec at a variety of source depths. A_R indicated by dot-dashed line, B_R by solid line, and C_R by dashed line.

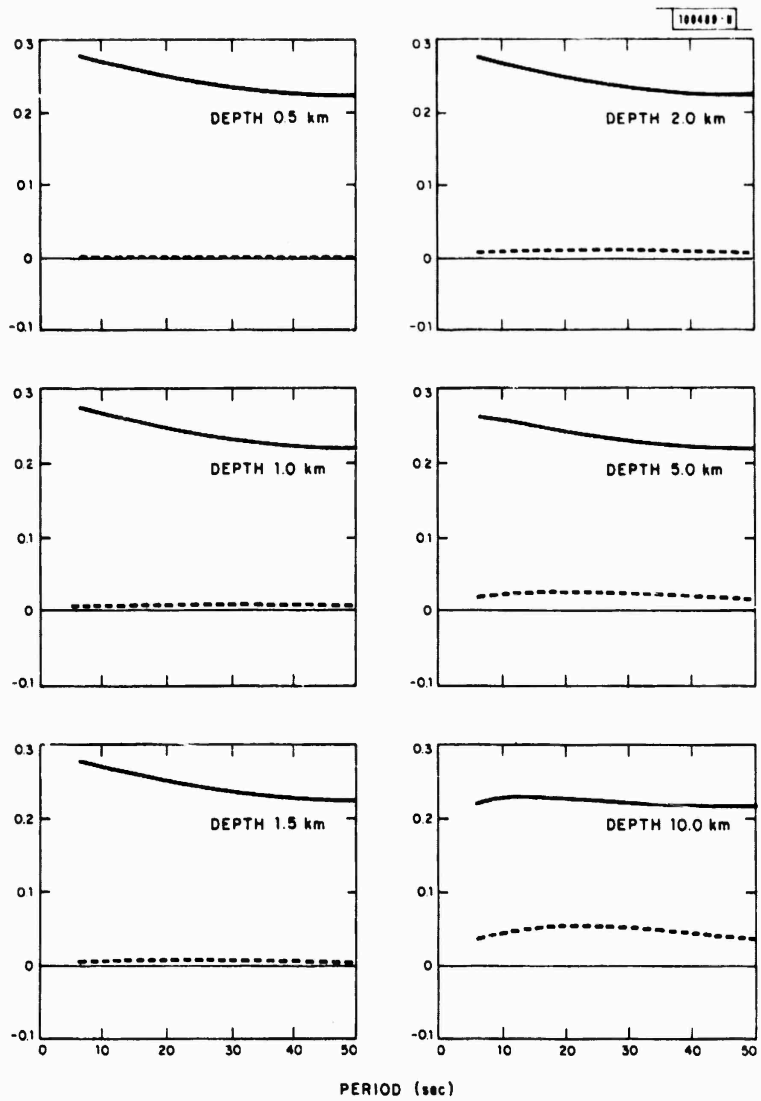

Fig. III-7. Values of A_L and B_L at a variety of source depths. A_L indicated by solid line, B_L by dashed line.

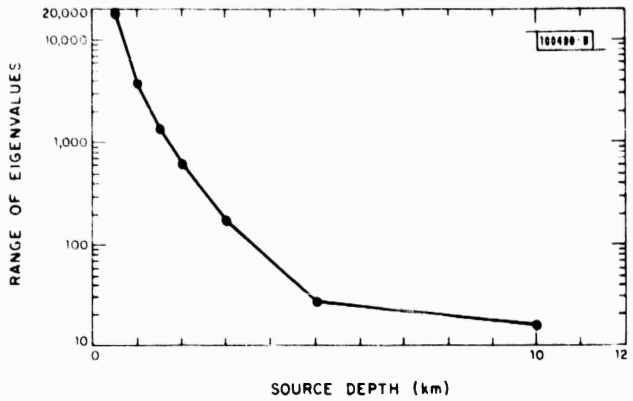

Fig. III-8. Range of eigenvalues obtained as a function of source depth at which synthetic data are generated.

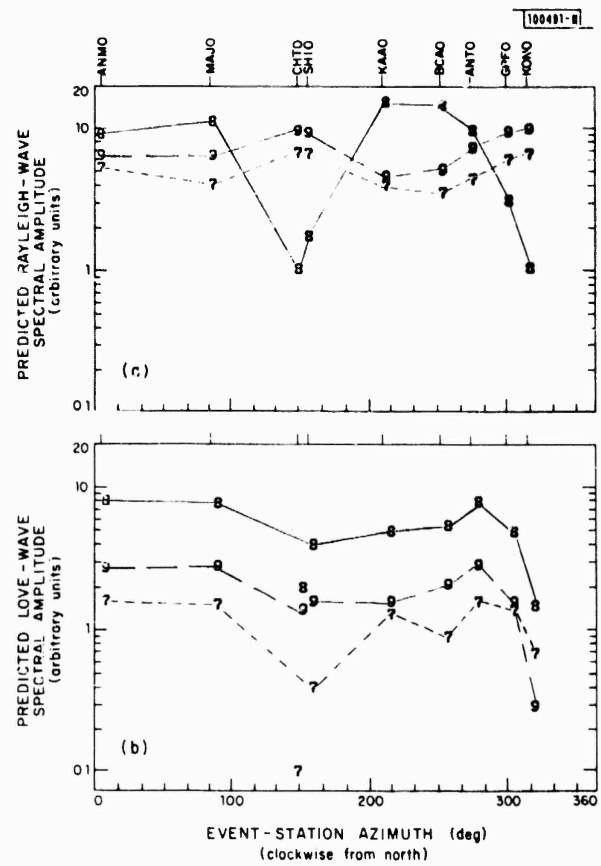

Fig. III-9. Variation of (a) Rayleigh-wave and (b) Love-wave spectral amplitudes with azimuth, as predicted from moment-tensor solution obtained for events 7, 8, and 9.

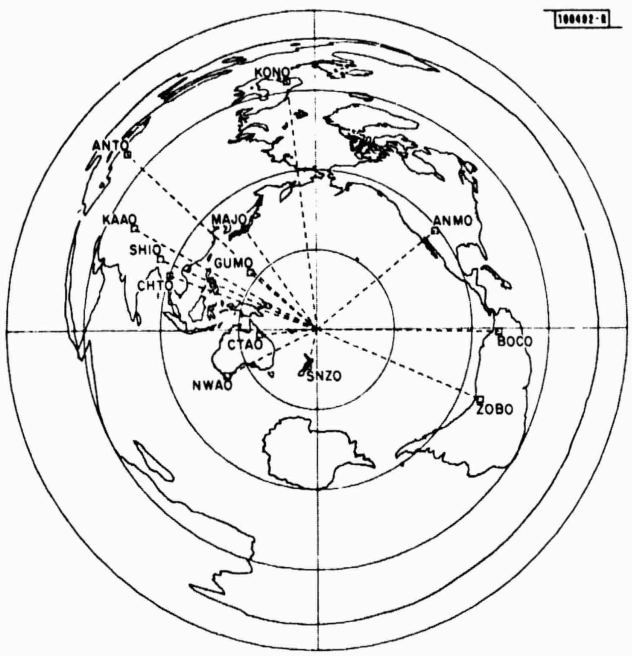

Fig. III-10. Distribution of SRO and ASRO stations used in analysis of event of 24 April 1979.

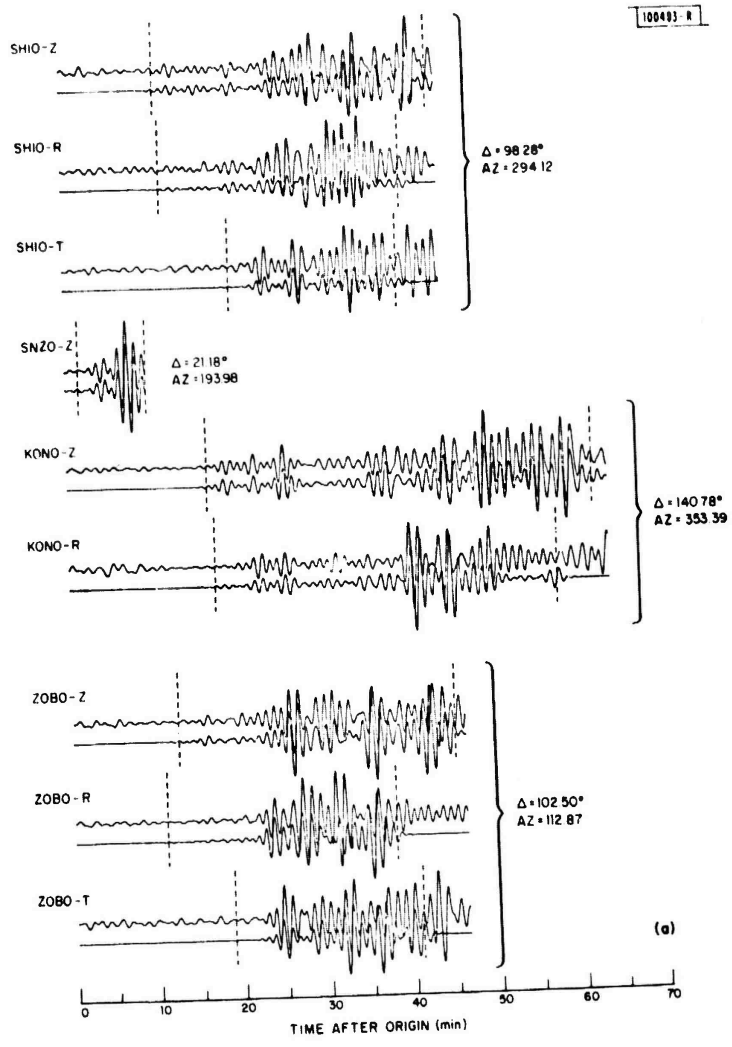

Fig. III-11(a-b). Deep (600-km) earthquake of 24 April 1979: comparison of observed and synthetic seismograms for selected stations. Scale for each component is arbitrary, but common to both observed and synthetic traces. Vertical dashed lines designate interval for which data were analyzed. Theoretical seismograms were not computed outside of that interval. Principal values and directions of axes (plunge/Az) are: (1) 2.1×10^{25} dyn-cm, 23/168; (2) 0.4×10^{25} dyn-cm, 5/76; (3) -2.5×10^{25} dyn-cm, 66/334; tension is positive. Notice glitch associated with P-wave arrival on record for station ANMO-Z.

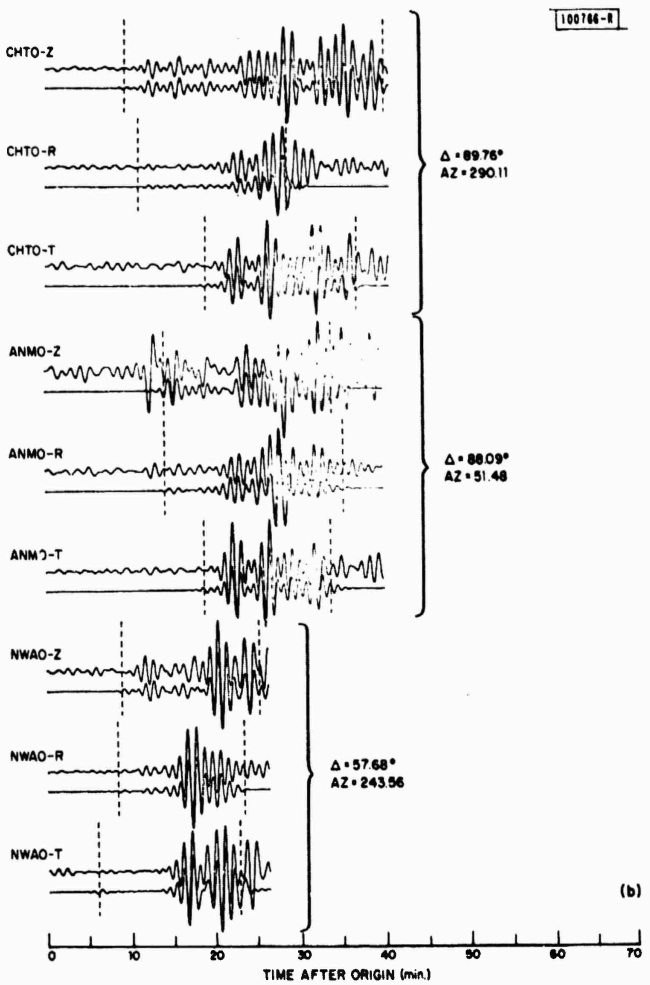

Fig. III-11(a-b). Continued.

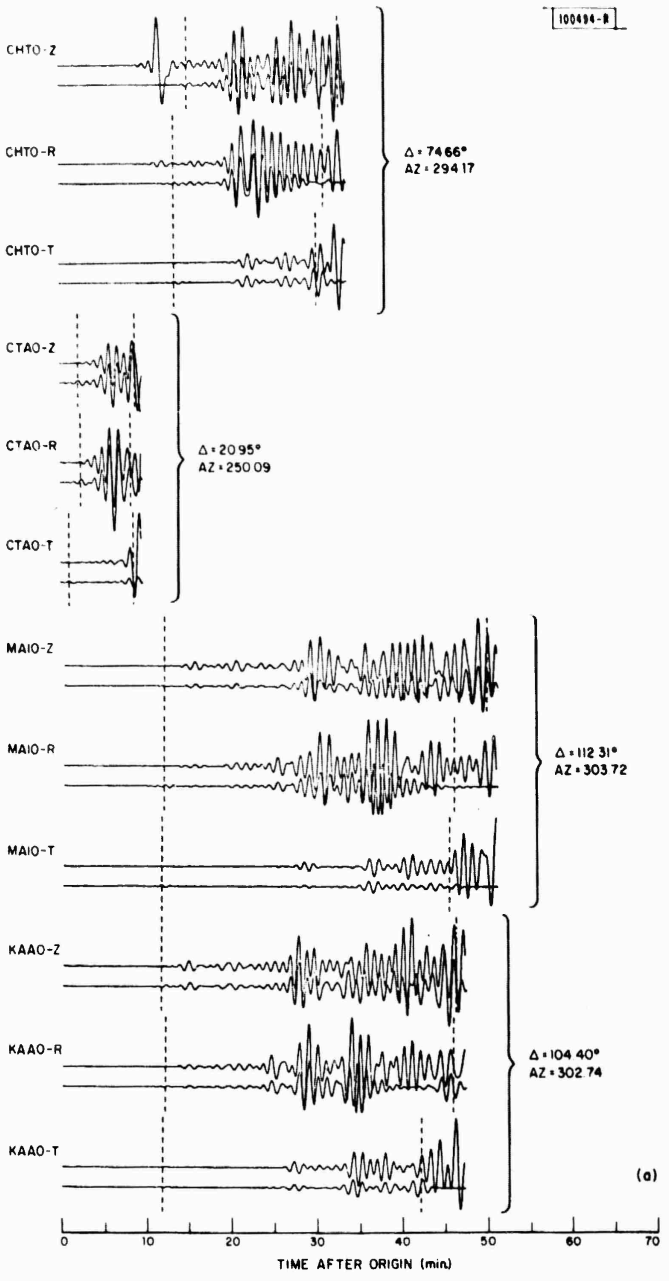

Fig. III-12(a-b). Same as Fig. III-11 but for event of 23 September 1978. Principal values and directions of axes (plunge/Az) are: (1) 1.4×10^{26} dyn-cm, 79/154; (2) 0.0 dyn-cm, 11/338; (3) -1.4×10^{26} dyn-cm, 0/248; tension is positive.

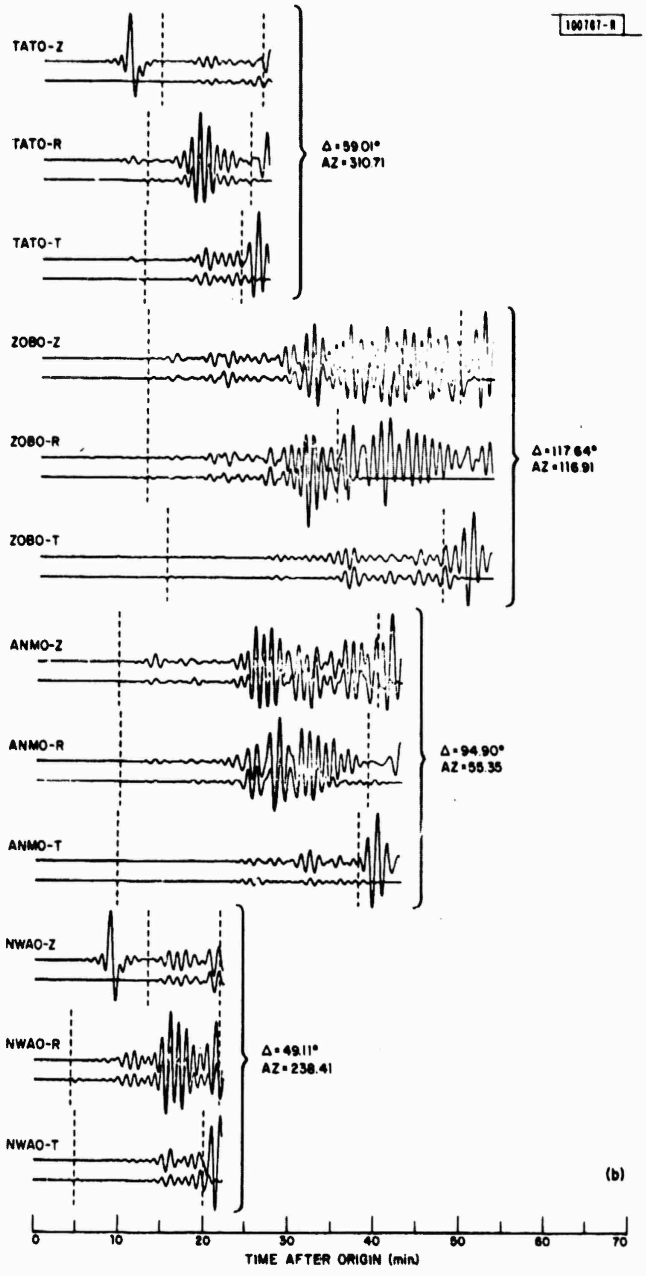

Fig. III-12(a-b). Continued.

IV. COMPUTER SYSTEMS

A. UNIX SYSTEM ENHANCEMENTS

Several efforts are being conducted to improve the computational support available to UNIX users at Lincoln Laboratory. The major projects are the installation of a new release of Bell Laboratories' UNIX operating system; coordination of software maintenance functions at existing UNIX groups within the Laboratory; and improvement of ARPANET software.

1. Installation of Seventh-Edition UNIX (V7)

We are presently completing installation of the seventh-edition release of the UNIX operating system (V7) on four computer systems: a PDP-11/45 and a PDP-11/50 used by Group 22 largely for computational support seismology research, a PDP-11/45 used by Group 24 for speech research, and a PDP-11/70 operated jointly by the two Groups. The V7 provides a number of features which were unavailable in previous releases. It is available for both the PDP-11 and the VAX CPU families, and permits substantially larger data sets than the previous versions. In addition, a number of bugs have been fixed and overall performance has been improved.

The user environment of V7 is also significantly improved. Bell provides a dialect of Fortran 77 which allows convenient mixing and interfacing of Fortran and C routines. A number of programs for performing routine data-processing tasks have been added and the text-processing package has been enhanced.

To speed the introduction of V7 programs and to smooth the transition to the new system, we made a few modifications to our existing sixth-edition (V6) kernel. The modified kernel provides the additional services required to execute user programs written for either V6 or V7. This has allowed us to run all of the V7 programs and still maintain access to the ARPANET, for which no V7 compatible software was available. Also, it has provided a period during which old programs continue to function and may be modified to run on a standard V7 system. As soon as final debugging of the V7 ARPANET software is finished, we will install the new kernel, which provides large file systems and other valuable although noncritical features.

2. Site Compatibility

The modified V6 kernel has been installed on the four existing UNIX systems at Lincoln. This has eliminated the growing divergence between the software at each site and has reduced the amount of duplicated effort expended in maintaining the systems. Since all software will run on any site without modification, corrections and enhancements done at any site may be quickly distributed to the other sites. This compatibility has been enhanced by the use of tables which define site-specific parameters (e.g., ARPANET host names). These parameters are read when programs are executed rather than being fixed at compile time. This substantially reduces the effort involved in distributing a program, while introducing no noticeable change in the program's performance.

3. New ARPANET Software

As the final phase of the conversion, the BBN ARPANET software is being modified to interface with the V7 kernel. This will correct many bugs in the earlier code obtained from the University of Illinois, as well as introducing the new 96-bit leader formats. This effort is in the

final debugging stages. When the installation is completed, the V7 kernel with network interface will replace the present modified V6 kernel at all sites.

K. J. Schroder

B. Graphpac

Graphpac is a package of over 40 subroutines and functions which are used to produce a graphics display on the Tektronix 4014 terminal. The routines can be called from both C and Fortran programs. Lower-level Graphpac routines include drawing a line from one point on the screen to another, moving the cursor from one point to another, outputting text, and erasing the screen. Higher-level routines include drawing linear- and log-scaled axes, plotting arrays of data, drawing polygons, and determining the position of the cross hairs. Graphpac was written to improve the speed of generating graphics, and to provide higher-level graphics functions. By not using a daemon, and sending output immediately to the user's terminal, speed was gained over existing graphics routines. The higher-level Graphpac functions have proved to be useful in several applications programs requiring axes, plotting of arrays, and other higher-level functions.

An important part of Graphpac is the concept of windows. The "uv window," set by the user, is a rectangular subset of the Tektronix screen. Once the user sets the uv window, he can draw and move the cursor in screen coordinates. A full-screen uv window has abscissas from 0 to 4095, and ordinates from 0 to 3119. However, the user's data values usually do not correspond with the values of the screen coordinates. The "xy window," set by the user, is the rectangular subset of the Cartesian coordinate plane where his data resides. Once the xy window and the uv window have been set, Graphpac will automatically map coordinates in the xy window to their corresponding values in the uv window. The user can specify whether the abscissas and ordinates in the xy window are linear or log scaled.

Graphpac also permits clipping to be performed. When clipping is activated, subsequent commands to draw lines will display only the portions of the lines which reside within the uv window. Portions of lines which are outside the uv window are "clipped" and not displayed. Coordinates in the xy window are first mapped to the uv window before clipping is done.

P. T. Crames

C. CONVERSION TO FORTRAN 77

Our Group has been bilingual with respect to programming languages since we began using UNIX. In general, Fortran is preferred by the seismologists because they are already familiar with it, have existing Fortran programs written for use on other systems, and would like to write in a language that is portable to other machines with a minimum number of changes. Most of the Group's programmers, on the other hand, prefer the standard UNIX language "C" because of its structured philosophy, ease of interactive use, flexibility, efficiency, and code compactness. The use of two languages for applications programs has resulted in frequent unnecessary duplication of existing software and necessitated the development of two versions of several subroutine packages, with the attendant difficulties of parallel maintenance.

Seventh-edition UNIX is supplied with a Fortran compiler that closely matches the new Fortran standard, commonly known as Fortran 77. This new compiler has the attractive feature of generating code that is compatible with the code generated from C. Interface subroutines were written in C for several libraries of subprograms having seismic applications, and a conversion

document was distributed which suggested equivalent alternatives to those features of Princeton UNIX Fortran which we had been using that would not work with the new compiler.

After considerable use, we have found that the new compiler is slower and produces much longer executable code because of a rather cumbersome implementation of formatted I/O; however, the advantages of C language compatibility, greater available program data space, better diagnostics, and a wider range of intrinsic functions make the use of the Fortran 77 compiler preferable for many applications.

D. A. Bach

GLOSSARY

AA	Automatic Association
ARPANET	DARPA Computer Network
ASRO	Upgraded HGLP Station
BBN	Bolt, Beranek and Newman, Inc.
CLVD	Compensated Linear Vector Dipole
CPU	Control and Processing Unit
DADS	Data Analysis and Display System
DARPA	Defense Advanced Research Projects Agency
DEC	Digital Equipment Corporation
HGLP	High-Gain, Long-Period (Station)
ISC	International Seismological Cen
ISDE	International Seismic Data Exchange
ISM	International Seismic Month
LRU	Least Recently Used
NMRO	Nuclear Monitoring Research Office
PDE	Preliminary Determination of Epicenter
SAS	Seismic Analysis Station
SATS	Semiannual Technical Summary
SDC	Seismic Data Center
SRO	Seismic Research Observatory
STAP	Short-Term Average Power
UNIX	(Trade-Mark) Bell Laboratories Operating System
USGS	U.S. Geological Survey
VSC	Vela Seismological Center
WMO	World Meteorological Organization
WWSSN	World-Wide Standard Seismograph Network

REPORT DOCUMENTATION PAGE

READ INSTRUCTIONS BEFORE COMPLETING FORM

1. REPORT NUMBER: ESD-TR-80-15	2. GOVT ACCESSION NO.: AD-A091107
3. RECIPIENT'S CATALOG NUMBER:	
4. TITLE (and Subtitle): Seismic Discrimination	5. TYPE OF REPORT & PERIOD COVERED: Semiannual Technical Summary, 1 October 1979 -- 31 March 1980
	6. PERFORMING ORG. REPORT NUMBER:
7. AUTHOR(s): Michael A. Chinnery	8. CONTRACT OR GRANT NUMBER(s): F19628-80-C-0002
9. PERFORMING ORGANIZATION NAME AND ADDRESS: Lincoln Laboratory, M.I.T., P.O. Box 73, Lexington, MA 02173	10. PROGRAM ELEMENT, PROJECT, TASK AREA & WORK UNIT NUMBERS: ARPA Order 512, Program Element No. 61101E, Project No. 0D60
11. CONTROLLING OFFICE NAME AND ADDRESS: Defense Advanced Research Projects Agency, 1400 Wilson Boulevard, Arlington, VA 22209	12. REPORT DATE: 31 March 1980
	13. NUMBER OF PAGES: 72
14. MONITORING AGENCY NAME & ADDRESS (if different from Controlling Office): Electronic Systems Division, Hanscom AFB, Bedford, MA 01731	15. SECURITY CLASS. (of this report): Unclassified
	15a. DECLASSIFICATION DOWNGRADING SCHEDULE:

16. DISTRIBUTION STATEMENT (of this Report)

Approved for public release; distribution unlimited.

17. DISTRIBUTION STATEMENT (of the abstract entered in Block 20, if different from Report)

18. SUPPLEMENTARY NOTES

None

19. KEY WORDS (Continue on reverse side if necessary and identify by block number)

seismic discrimination	surface waves	NORSAR
seismic array	body waves	ARPANET
seismology	LASA	

20. ABSTRACT (Continue on reverse side if necessary and identify by block number)

This report describes 19 investigations in the field of seismic discrimination. The contributions are grouped as follows: 6 describe progress in the development of a Seismic Data Center; 3 describe research into seismic algorithms that will be implemented at the Data Center; 7 are concerned with the problem of source characterization using the seismic moment-tensor formulation; and 3 describe recent improvements in our in-house computer systems.